EXPERIMENTAL INVESTIGATION OF MINICHANNEL HEAT SINKS FOR ELECTRONIC COOLING APPLICATIONS

by

VIJAYARAGHAVAN VEMBULI

A thesis submitted to the

Graduate School-New Brunswick

Rutgers, The State University of New Jersey

In partial fulfillment of the requirements

For the degree of

Master of Science

Graduate Program in Mechanical and Aerospace Engineering

Written under the direction of

Dr. Yogesh Jaluria

And approved by

_____

_____

_____

New Brunswick, New Jersey

MAY 2015

ABSTRACT OF THE THESIS

Experimental Investigation of Minichannel Heat Sinks for Electronic Cooling Applications

by VIJAYARAGHAVAN VEMBULI

Thesis Director:

Dr. Yogesh Jaluria

Several novel methods of fabricating heat sinks have been developed in recent years, with complicated profiles. However, in this study, we focus on the conventional machining technique to fabricate simple, geometrically enhanced heat sink with readily available, less expensive, liquid such as distilled water, which still have potential to be explored further. There has been a lot of work done with heat sinks on the mini scale (diameter often to the order of 1 mm). So it was decided to explore some simple geometries of heat sinks with available tools for machining. The heat sink material was chosen as brass. Three different straight channel heat sinks were fabricated, using conventional milling process, of width 2 mm, 3 mm and 4 mm, respectively. The height of the channel is kept constant at 4mm. The heat generated by an electronic component was simulated by an Omega Kapton flexible heater. At a heat power of 12 W, the lowest heat sink base temperature was achieved using the 2mm heat sink. Also, the pressure drop across the heat sink has been reported. The temperature drop across the heat sink has

been reported and it has been found to be maximum for a heat sink with 2 mm fin spacing. Base temperature of the heat sink was found to decrease by reducing the width of the channels and by increasing the flow rate of distilled water over a period of time. It can be concluded from the experimental investigation that the geometrically enhanced heat sinks manufactured using conventional methods is comparatively less expensive.

ACKNOWLEDGEMENTS

I would like to extend my sincere gratitude to my advisor Dr. Yogesh Jaluria for the constant support, guidance and encouragement towards my thesis. He has been such a great inspiration and I really thank him for giving me this opportunity to work on this project. I am deeply thankful to him for the moral support during difficult times and for his great patience. I will cherish all the invaluable advises that he has given me and the conversations that we've had, for the rest of my life.

I also would like to thank Dr. Mona Zebarjadi for believing in me and giving me an opportunity to work in her project. I am really proud to be one of her first graduate students. It's been absolute pleasure working with her. I would like to thank Dr. Keivan Esfarjani for helping me while I was working with Dr. Zebarjadi. Special thanks to Dr. Javier Diez who has been a great mentor and friend. I am very glad that I got a chance to take his class and I sincerely thank him for accepting my request to be in my thesis committee.

I have no words to express my gratitude to Mr. John Petrowski. He is one of the kindest person I've ever met. He has helped me since design stage to fabrication and during investigation. He has been a pillar of support for my project. I sincerely thank him for all the help and support he has provided me. I'd like to thank Mr. Joseph VanderVeer for his valuable inputs and help with my experiment. One of the most important acknowledgements goes to my lab partners Sunny Wong, Dr. Meng for all the guidance and support on my project.

Last but not the least; I would like to thank my dad and mom for all the moral, financial support and for always believing in me. I would also like to dedicate this work to my late grandmother who has been great inspiration all my life.

Contents

LIST OF FIGURES

LIST OF TABLES

NOMENCLATURE

A	Area, m^2
C_p	Specific heat (kJ/kg °C)
D_h	Hydraulic diameter (m)
E_u	Euler Number- $\frac{P_{high} - P_{low}}{\rho V^2}$
f_f	Friction factor
h	Heat transfer coefficient (W/m^2 K)
k	Thermal conductivity (W/ m K)
L	Length of the channel (mm)
Nu	Nusselt Number - $\frac{h D_h}{k}$
P	Power Density (W/ m^2)
ΔP	Pressure Drop (Pa)
q	Heat flux (W/ m^2)
Q	Flow rate (m^3/ s)

r_h	Hydraulic radius (m)
Re	Reynolds number - $\frac{\rho V D_h}{\mu}$
T_{out}	Temperature of coolant at the outlet (°C)
T_{in}	Temperature of coolant at inlet (°C)
T_{base}	Base Temperature of heat sink (°C)
u	Velocity (m/s)
V	Characteristic Velocity of the Flow (m/s)
W	Width (mm)

Greek Symbols

Δ	Difference
μ	Dynamic Viscosity (kg/ m-s)
ϑ	Kinematic Viscosity (m^2/s)
θ	Dimensionless Temperature
β	Thermal expansion coefficient (K^{-1})
ρ	Density (kg/m^3)

Subscripts

f	Friction factor
in	Inlet
out	Outlet
h	hydraulic radius or diameter

Chapter 1 **Introduction**

1.1 Motivation

Thermal management of electronic devices has gained more importance than ever before due to the recent advancements in computing power. The scale of the devices has come down to micro/Nano scales, which promote high end performances for such devices. So thermal management of such high performance devices becomes crucial. Previously, in our group, Dr. Jingru Zhang had fabricated several profiles of microchannel heat sinks targeting high heat generating microprocessors and other energy consuming applications. Micro scale heat transfer properties of those profiles were investigated and published. Her work on micro channel heat sink fabrication has been a source of motivation. Since our group has already worked on micro scale heat transfer sinks, it was decided to scale up and explore some simple configurations on a mini scale.

The main agenda of this study is to investigate the thermal performance of a proposed electronic cooling system. Mini-scale electronic cooling was studied through experiments focusing more on the moderately heat producing devices and applications. Three different configurations of minichannel heat sinks were designed, fabricated and investigated. Several limitations have been analyzed and it has been considered during the design phase of the heat sink for convenience. There has been a lot of work done on minichannel heat sink fabrication with various working fluids, but not many studies focused on conventional milling method due to the limitation with respect to the milling tools that are currently available and the capacity of the machine shop that you are going to use for fabrication. The thesis starts with the brief review on the previous work done with similar interests in minichannel heat sink fabrication. Then we discuss about the design concepts, materials used and experimental setup. Various

devices used to measure the data are discussed in detail along the experimental setup. Results are discussed following experimental set up and conclusions with scope for future work is explained at the final chapter.

1.2 Literature Review

A numerical investigation on the heat transfer characteristics of water cooled minichannel heat sinks was performed by Xie et al (2007). It was concluded from their investigation that heat removed by a heat sink increases by decreasing the channel width of the minichannel while the thermal resistance increases by increasing the channel width. In the investigation conducted by Mudawar et al (1994) two phase cooling for electronic chips was explored by the application of flow boiling in minichannel. It was concluded that minichannel geometry was determined to offer inherent advantages over the micro channel geometry whereas the latter is preferred only in places for dissipation of high heat fluxes where minimizing weight and liquid inventory is a must.

Recent work on water cooled minichannel heat sinks for microprocessor cooling by Saad et al (2013) provided a great insight on the geometric effects on cooling for straight minichannel. They fabricated five different heat sinks with fin spacing's of 0.2 mm, 0.5mm, 1.0 mm, 1.5 mm along with a flat plate heat sink were investigated. As a result of their investigation the base temperature and thermal resistance of the heat sinks were found to drop by decreasing the fin spacing and by increasing the volumetric flow rate of water circulating through the heat sink. The cost and ease of manufacturing aspect of liquid cooling system investigation was conducted by Whelan, Kempers and Robinson (2012) . This new block based on miniature jet stream design performed better than commercially available cooling block. An experimental analysis was conducted by Naphon and Wongwises (2010) on the jet liquid heat transfer characteristics of

the mini rectangular fin heat sink of a CPU based on real processor operating conditions and they concluded that the use of jet impingement cooling system resulted in a lower CPU operating temperature when compared to conventional liquid cooling system. Following this investigation an intermittent multi jet spray system for cooling of microprocessor was employed by Panao, Moreira, and Durao (2012). And Bower et al (2003) tested Extrusion free form fabricated SiC carbide mill-channel heat sinks. The overall heat transfer coefficient for a single row of SiC heat exchanger compared favorably with copper equivalents however the heat transfer coefficient in multiple row heat sinks did not agree well with the laminar theory.

Another aspect of thermal management in electronic cooling is enhanced liquid cooling that has been investigated by enhancement of the thermo physical properties of the liquids. Eastman et al (2001) reported around 40 % enhancement in thermal conductivity as a result of 0.3% loading of copper nanoparticles in ethylene glycol. Similarly Choi et al (2001) also reported an anomalous enhancement of 160% in thermal conductivity with a volume concentration of 1% of Multi walled carbon Nanotube. Several works has indicated from the literature that Nano fluids gives better heat transfer performance. The performance of Al_2O_3-water Nano fluid in commercial liquid cooling system was investigated by Roberts and Walker (2010) who reported an enhancement of 20 %. The main observation was that the nano liquids gained more temperature than water passing through the same cooling block for the same heat flux. Some important results on turbulent conditions were reported by Nguyen et al (2005) there was a greater decrease in the junction temperature as compared to the laminar flow regime when ethylene glycol based nanoliquids has been used. There has been an investigation of diamond Nano fluids with 1% volume loading which resulted in reduction of temperature difference between the evaporator and the condenser. It's been quite clear from the literature review that researchers have used either commercial minichannel with nanofluids or pure liquids to reduce

the microprocessor temperature. There's been some issues reported using the nanofluids like more maintenance, cost, aggregation and deposition in the heat sink. Also almost few researchers tried to explore the sink geometry to enhance the heat transfer characteristic. Though some of them tried to go below 1 mm channel width or fin spacing they did not try fabricating a sink with conventional machining method. So we wanted to explore the systematic effect of sink geometry on reducing the temperature of the computer processor like devices.

1.3 Dissertation Outline

Chapter 1 gives a brief overview on the motivation of this project. It gives us a picture on the recent trends and need for efficient cooling of the electronic devices on macro scale and micro scale. Literature review is briefly discussed and subsequently the purpose of this study is established. By reviewing the literature we can understand how this study differs from the rest of the investigation that has been done for similar applications.

Chapter 2 describes the design aspects of the mini-channel heat sink under investigation. Several configurations and dimensions are discussed in detail. CAD drawings are presented with dimensional constraints on the substrate. Detailed descriptions on the entrance length, substrate thickness are discussed. Basics of milling process are discussed briefly.

Chapter 3 presents the experimental configuration. More details on the experimental set up, various devices used, calibration of the devices used to collect data and finally uncertainty analysis is presented.

Chapter 4 Several dimensional and dimensionless parameters are briefly explained. Various property tables are introduced. Experimental results are discussed briefly. The thermal

performance of all the three configurations of heat sink and fluidic performance of the heat sinks are explained.

Chapter 5 provides the conclusions of this study. Different configurations are summarized following the results from the experimental investigation. Further scope for improvement on the current design, fabrication method and on the working liquid with possible modifications and outcomes are discussed.

Chapter 2 **Design and Fabrication**

2.1 Design of Minichannel heat sink

The first stage of any investigation is the design stage. It is important that we should contemplate different ideas, configurations with different features before we fabricate. Design stage offers the flexibility and robustness to make quick changes before fabricating a substrate. After various stages of development and discussion we decided the overall dimension of the substrate to be $70\,mm \times 50\,mm \times 8\,mm$ based on various previous works, literatures and considering the ease of the fabrication. After excluding the walls and entrance length of the substrate the effective dimensions of the minichannel would be $50\,mm \times 40\,mm \times 4\,mm$. Three different widths of straight minichannel were designed with additional features that facilitates better and accurate recording of data. Following table includes various dimensions like height, width and wall thickness between the channels for three different configurations of straight channels.

Table 2.1 Dimensions of Heat sinks

Channel Width (mm)	Height (mm)	Wall Thickness (mm)	Number of Channels
2	4	1	10
3	4	1	8
4	4	1	7

2.1.1 Design of 4 mm Minichannel

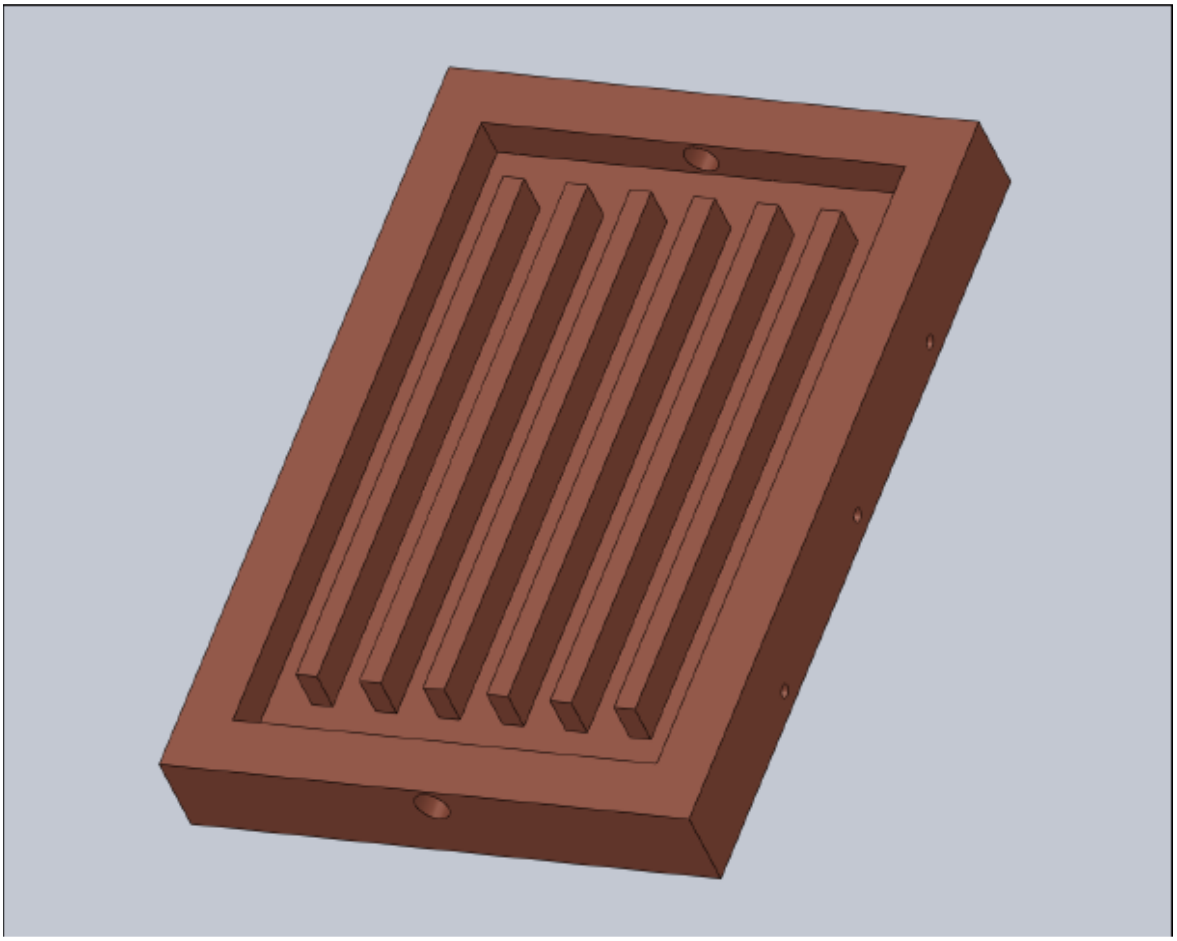

Figure 2.1: **3D- Drawing for the 4mm Minichannel heat sink**

Design investigation was carried out using Solidworks design software for creating a 3-D model for all the three configurations. It is fairly simple to draft a 2-D design from a 3-D model. This design provides us the basic details and insight about the 4mm heat sink. The dimensions for different segments of the heat sinks and additional features are depicted more clearly in the 2-D draft of the 4mm minichannel heat sink substrate.

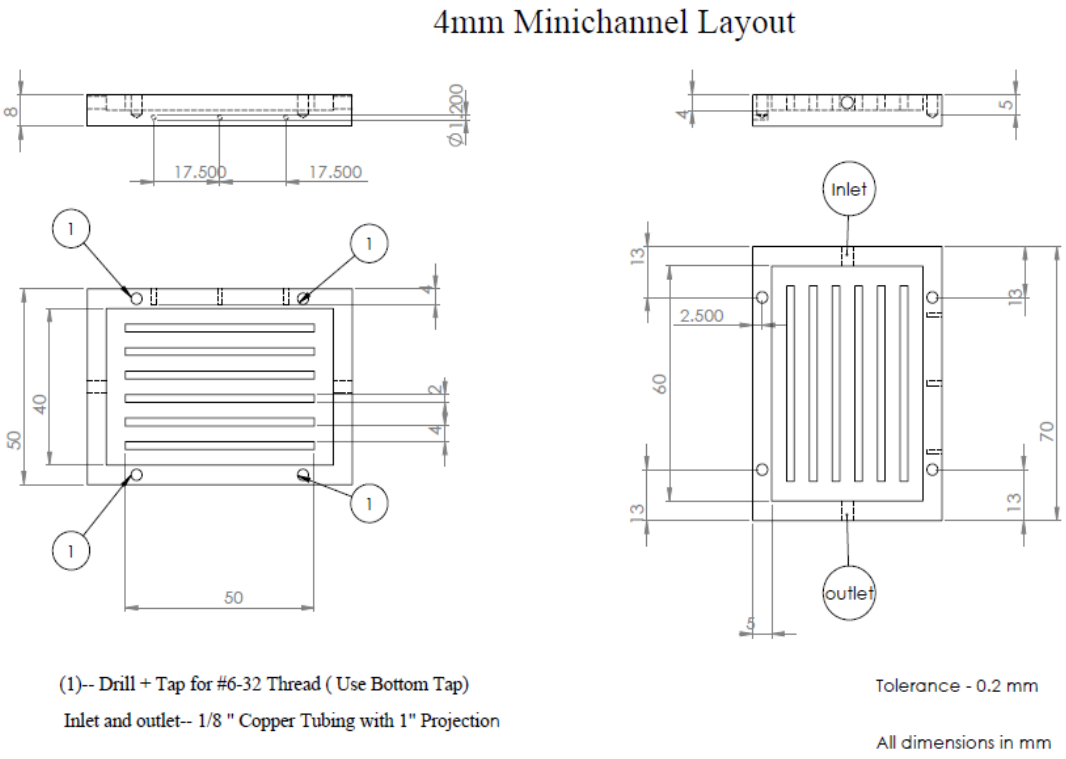

Figure 2.2: **Two Dimensional Draft of 4mm minichannel heat sink**

The two dimensional draft for the 4mm channel shows various dimensions that are crucial and needs to be analyzed before moving on to fabrication. The outer wall thickness of the substrate remains 5 mm on all the sides. The overall length of the wall which typically denotes the length of channel is considered to be 50 mm. As we can conclude that the overall thickness of the substrate is 8 mm and the height (or depth) of channel is taken as 4mm. An entrance region was introduced for 5mm from the inlet. The main reason for introducing such entrance region distance was to ensure uniform and distributed flow through all the channels especially at higher flow rates. For similar reason an exit region distance is provide before the outlet. There are four #6-32 threaded holes were mentioned. This is to secure the heat sink with a cover with a seal to ensure there is no overflow from any possible vents between the cover the heat sink surface. The inlet and outlet have a 1/8 “NPT copper tubing for supply of coolant from a syringe

pump. Also we notice that there are three holes that penetrates 4 mm deep from one of the sides and the diameter of the holes are 1.2 mm from the bottom of the substrate. These holes enable us to calculate the base temperature of the heat sink at three different lengths, from which we can find the mean base temperature of the heat sink.

2.1.2 Design of 3 mm Minichannel

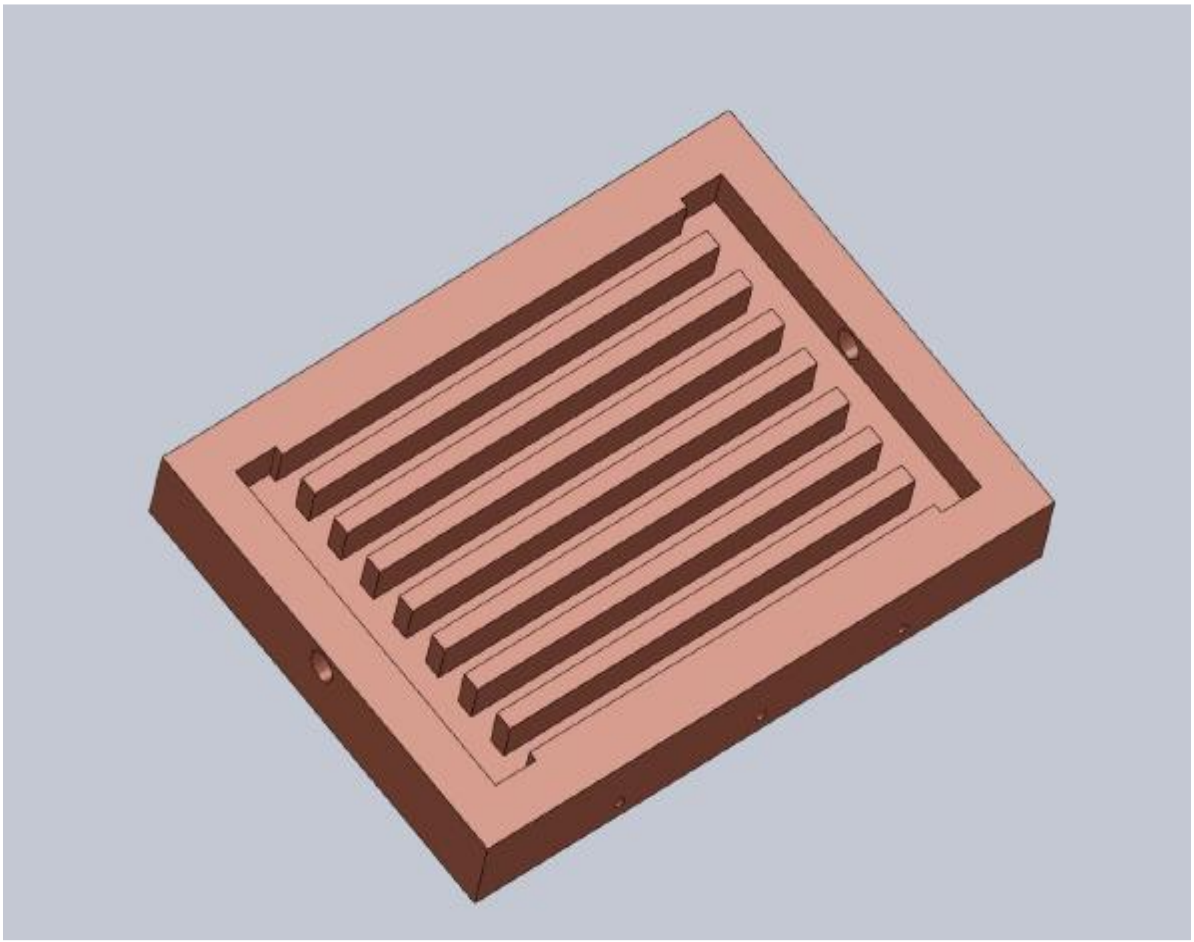

Figure 2.3: **3D- Drawing for the 3mm Minichannel heat sink**

After designing the 4 mm minichannel heat sink we decide to reduce the width of the channels by 1 mm and subsequently we ended up have a this profile. With the same substrate area we have reduced the width of the each individual channel by 1 mm to get one more channel. Previously on the 4 mm channel we ended up having seven channel whereas in this case we have an additional 8th channel. Otherwise the distance of the channels from the inlet and the distance to the outlet are all the same as in the previous design. But you can find that the end channels are surrounded by a protruded wall (or fin) on one side unlike the first configuration.

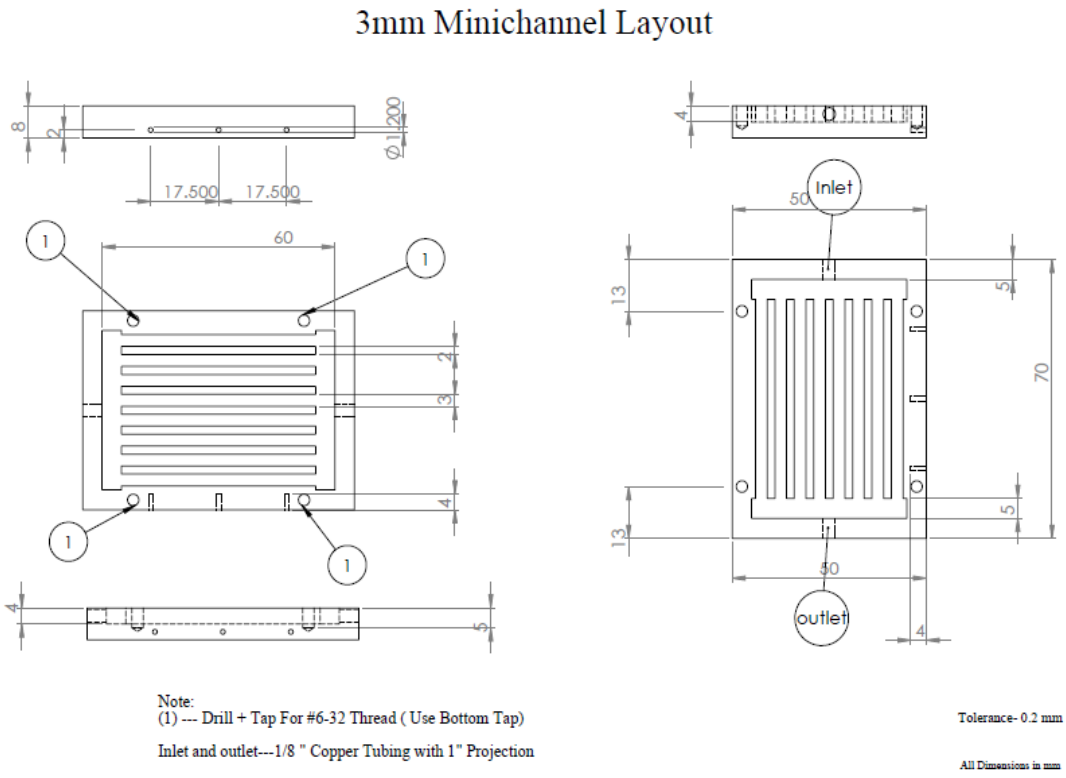

Figure 2.4: **Two Dimensional Draft of 3mm minichannel heat sink**

This presents the two dimensional draft drawing for the 3 mm minichannel heat sink. All the dimensions considered for fabrication is more or less the same from the 4 mm channel design except the width. Also it is important to pay attention to the closest tolerance to the radius of curvature we could attain for this profile that consists of a protruded wall at the ends. The overall outer wall thickness of the substrate remains the same as 5 mm as in the previous design.

2.1.3 Design of 2 mm Minichannel

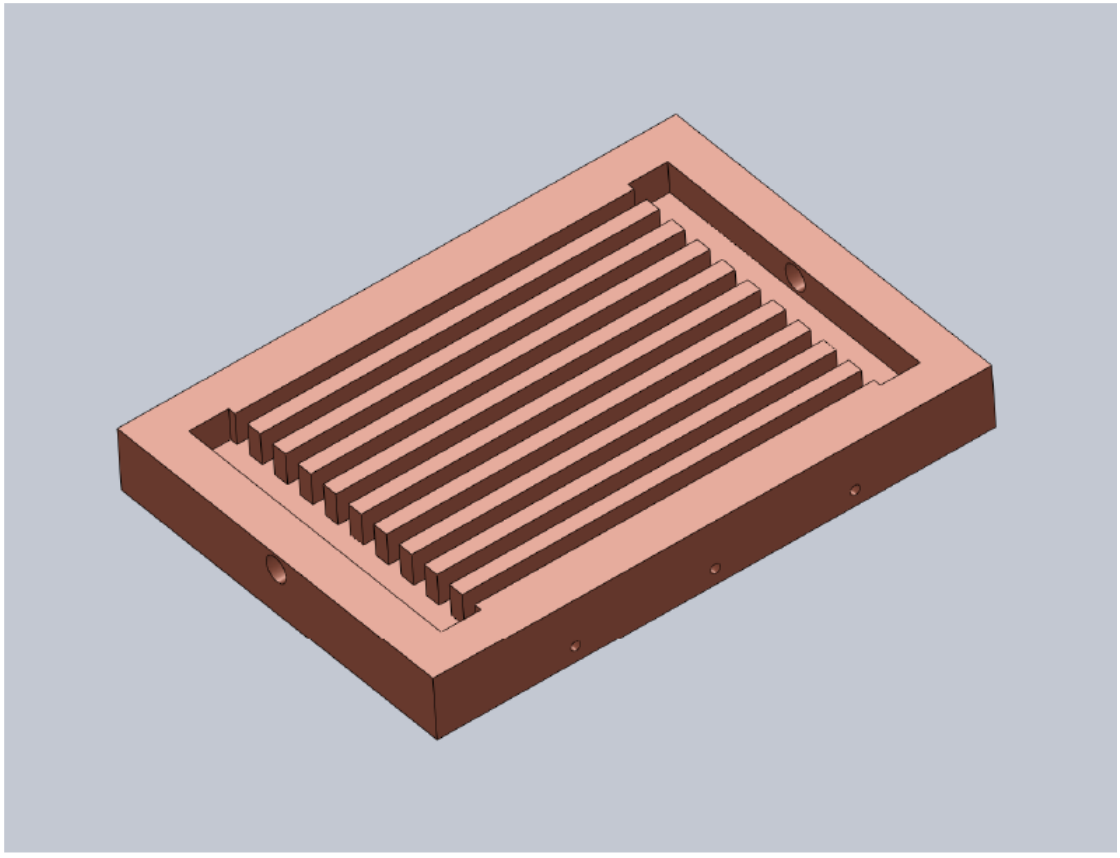

Figure 2.5: **3D- Drawing for the 2mm Minichannel heat sink**

The three dimensional drawing presents the configuration of the 2 mm minichannel heat sink. It is evident that this configuration contains more number of channels than the previous configurations after reducing the width of the channel. But the height of the channel and wall thickness remain the same at 4 mm and 1 mm. The length of the channel and other dimensions remain unchanged.

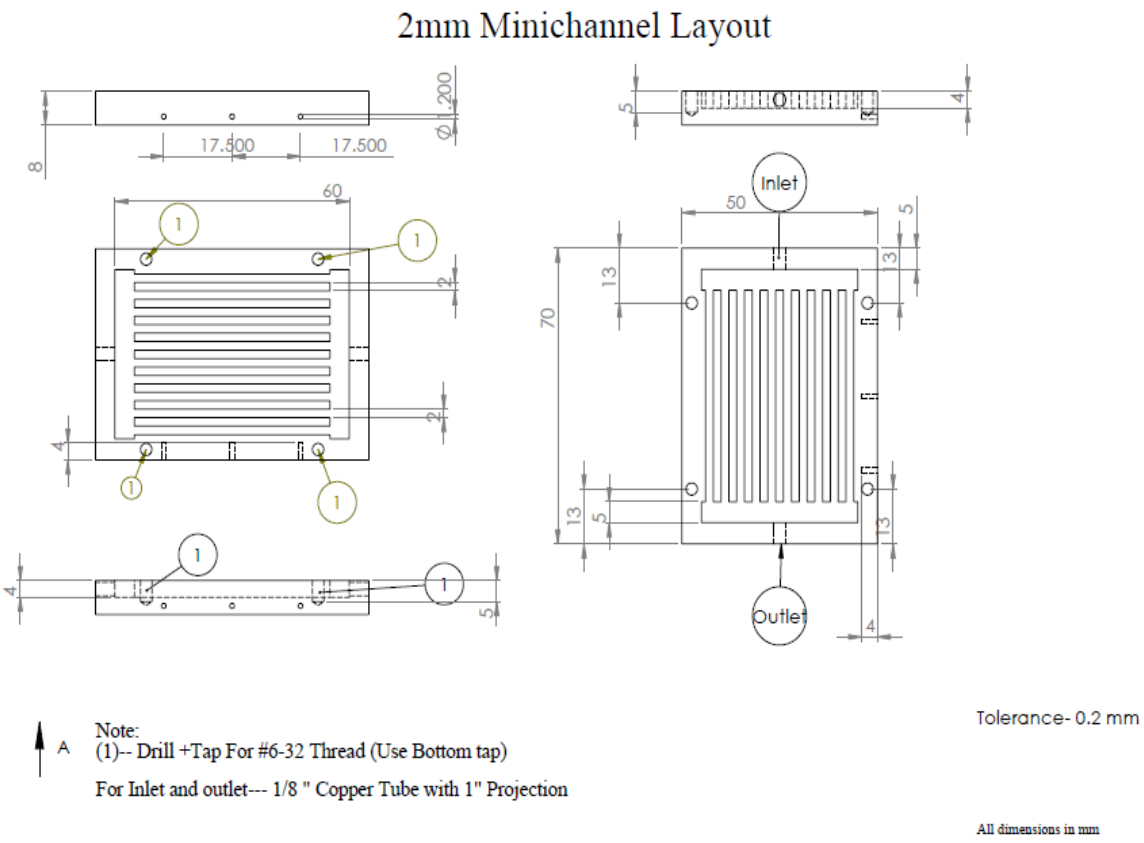

Figure 2.6: **Two Dimensional Draft of 2mm minichannel heat sink**

2.2 Material

2.2.1 Material Selection

There are certain limitations with materials with conventional milling machining method. So it is important that we choose the option with the ease of machinability as well as good thermal, mechanical properties. From the machinability aspect we shortlisted alloys of copper and aluminum. Since the working fluid is decided to be distilled water we had to eliminate aluminum in spite of good mechanical properties because of the fact that aluminum develops a thin layer of aluminum oxide of a few millimeters that prevent it from reacting with water. So it is quite evident that aluminum is not a suitable option when you are using liquid coolant like water. So we had to choose copper. There are different alloys of copper which is commercially available with good machining and thermal properties. Following are the property table for two different alloys that was being considered.

Table 2.2 Property table for copper alloys

Alloy	Copper (Cu) (%)	Tensile Strength (psi)	Yield Strength (psi)	Machinability Rating (%)	Thermal Conductivity (W/m K)
Copper 110	99.9	32000	10000	20	338
Copper 360	61.5	58000	45000	100	110

As you can find from the properties table that both copper 110 and copper 360 have varying properties and we had to choose carefully after careful considerations pertaining to the current study. The percentage of copper is high in copper 110 which is one of the most pure form of copper available in the market. Because of the higher copper content, copper 110 has excellent thermal and electrical conductivity properties. But has very poor machinability rating. Meanwhile the thermal conductivity of copper 360 alloy is comparatively less but it has great machinability properties. Apart from these reasons corrosive properties of both the alloy was investigated and it was reported that brass (copper 360) which is used in commercial piping and other applications is favored over the more pure form copper 110. Copper 110 has poor machinability under such precision machining conditions and more corrosive with liquids like water. So after brief investigation we decided to use copper 360 alloy (brass).

2.3 Fabrication

2.3.1 Introduction to Milling

Milling is the process of cutting away the material by feeding a work piece past a rotating multiple tooth cutter as explained in the tutorial of PowerMill [23]. The cutting action of many teeth around the milling cutter provides a fast method of machining. In the present scenario several configurations of tools exists. Some machines have the table/ work piece stationary whilst the X, Y and Z axes move and others may be constructed to allow the work piece to be the moving part while the axes are fixed. In any conditions X, Y and Z axes directions are configured the same.

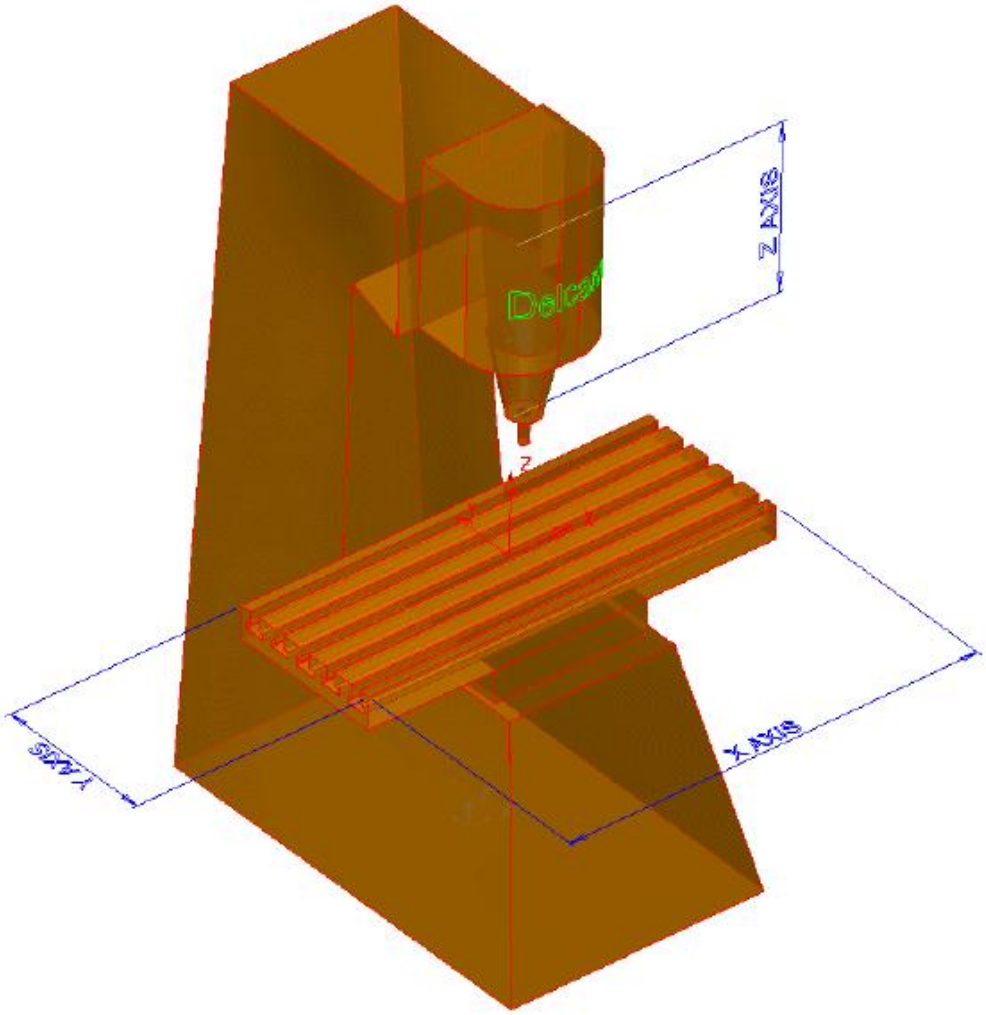

Figure 2.7: **Milling machine with showing the axis of operation [23]**

- The X- axis is considered to be the longest axis, where X+ will be the table motioning to the left and X- to the right.
- The Y-axis moves from front to back of the machine with the table motioning towards the operator as the Y+ (positive) direction and away being the Y- (negative) direction.
- The Z-axis where the tool normally is located has the Z+ (positive) axis motioning up and away from the work piece and Z- (negative) direction towards the work piece.

Some machine tools possess further access to allow great versatility when machining complex components. We can add a fourth axis like rotary table or a five axis configuration. Both can either be manually set up (operator controlled) and computer controlled. CNC milling is quite popular with recent advancement software's and control equipment. Three axis motions normally involve linear motion along three principal directions with the tool being at the same orientation for every motion.

2.3.2 Methods of Milling

There are generally two methods of milling, climb and conventional.

Climb milling is sometimes referred to as down milling, where the direction of the cutter rotation is same as the feed direction. This method is common the on the shop floor and will often produce a better surface finish.

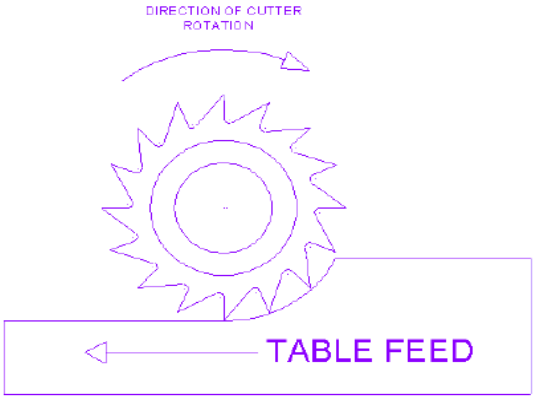

Figure 2.8: Climb Milling [23]

Conventional milling is also referred to as up milling where direction of the cutter opposes the feed direction.

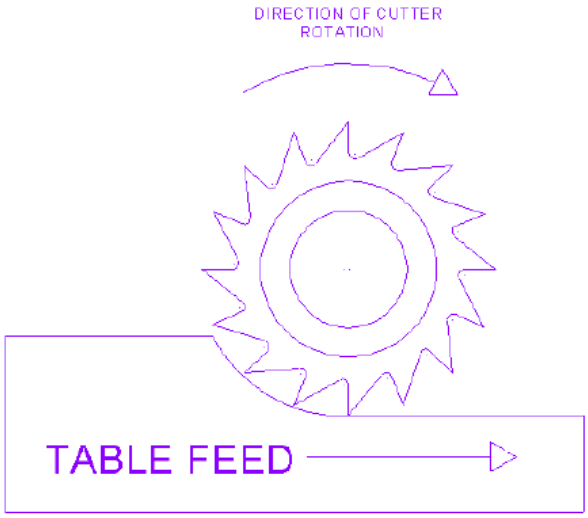

Figure 2.9: Conventional Milling [23]

2.3.3 Tolerance and Thickness

Suitable values are required to control the accuracy and amount of excessive material to be left on the component by a toolpath. The parameters used for this purpose are preset and are called Tolerance and Thickness. There are two independent locations for setting these values depending on whether the programmer is performing a roughing or finishing operation. The tolerance controls the accuracy that to which the cutter path follows the shape of the component. It can be above or below the stated thickness value. The thickness is the amount of additional to remain on the component surface after machining. This amount would vary depending on the current tolerance. Another term worthwhile mentioning in the milling process is step over. It is defined as the distance a tool moves between the adjacent toolpath tracks. The

distance or the step over value determines whether the surface on a component is rough or smooth. When using a flat bottomed tool like End mill the step over value normally ranges around 70% of the cutter diameter. This is one of main reason for fixing the height of the channel for all the three configurations as 4 mm. Also the milling tool to mill a channel width of 2 mm channel, the cutting length was around 5-6 mm. The above width and height of the channel gives us a good tolerance limit while milling. Also the radius on the corners accounts to 0.0682 mm, since it's difficult to get a perfectly square ends while milling with an end mill tool.

(2.10) Fabricated 2 mm channel

(2.11) Fabricated 3 mm Channel

(2.12) Fabricated 4 mm Channel

Chapter 3 **Experimental Procedure**

3.1 Laminar Vs Turbulent Flow

There are three different flow regimes for a working fluid flowing in a channel. These are laminar, transitional and turbulent region. The flow regime can be related to the Reynolds number:

$$Re = \frac{\rho V D_h}{\mu}$$

Whereas the hydraulic diameter is defined as: $D_h = \frac{4A}{P}$

Reynolds number is the ratio between inertia force and viscous force. When Reynolds number is greater than 4800, then the flow is turbulent. Reynolds number between 2100 and 4800 corresponds to the transitional regime which denotes that the flow is in transition to the turbulent regime. Stream line offers a best description for a flow. The streamlines of turbulent flow are chaotic in nature as shown by Osborne Reynolds [11], where he injected dye through a glass tube that enabled him to view the nature of flow at different flow characteristics. With Reynolds experiment, it was discovered that turbulent flow has velocity fluctuations that causes the streamlines to move in an erratic matter. Which in turn allows the dye to be dispersed in the flow.

However the streamlines for a laminar flow is smooth and steady. In fully-developed laminar flow the velocity profile is parabolic. The Reynolds number that is needed to maintain a laminar

flow is normally under 2100. This occurs with the combination of high viscosity, low density and tube diameter.

3.2 Laminar Flow Friction Pressure Loss

The friction factor is useful to determine the pressure drop at different flow regimes. The Equation for friction factor in fully-developed laminar flow is $f_f = \frac{64}{Re}$. This can be found using the Moody chart, which uses Reynolds number to find different friction factor for various surface roughness.

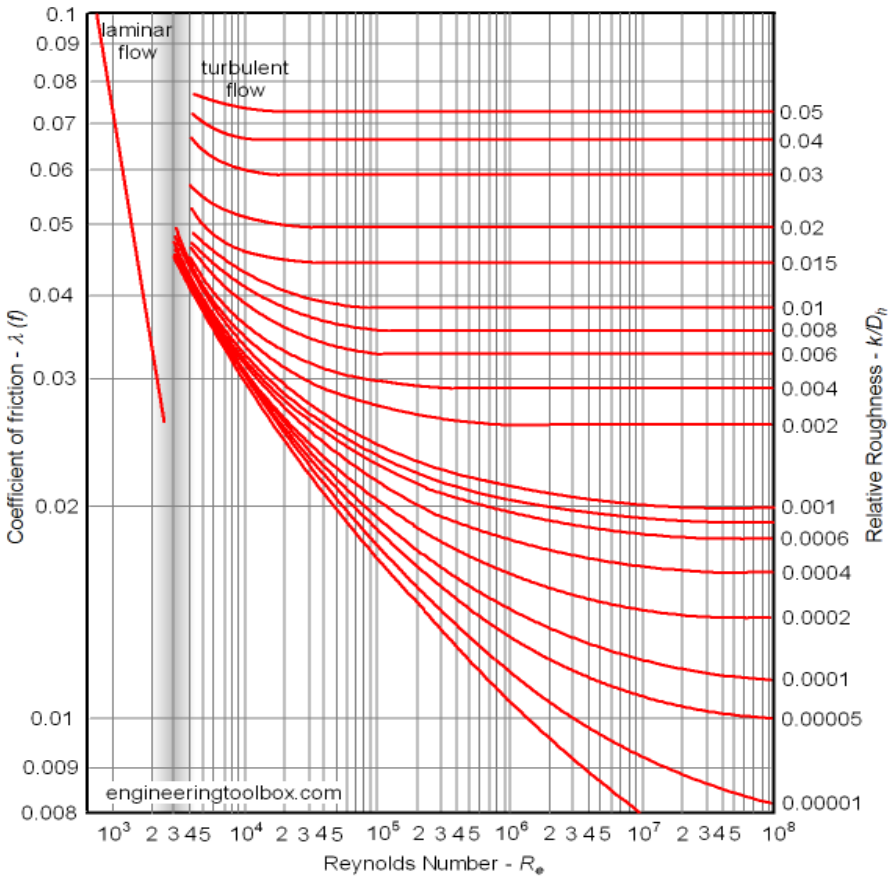

Figure 3.1: Picture of Moody Chart [Engineering Toolbox (24)]

The main objective of this study is to measure the thermal performance of the heat sinks by measuring the temperature drop at various flow, however we deal everything in the laminar regime. The design of experiment and capacity of the flow pump allows wide operating range within the laminar region.

3.3 Experimental Setup

The experimental set up consists of various key elements to successfully run the investigation of the fabricated heat sinks. These include data acquisition system, thermocouples, syringe pump, variable AC to DC power supply which acts as the source of constant heat flux for the heat sink and pressure transducer and DC current sources for the transducer. The flow loop in this study is designated as an open loop as shown below.

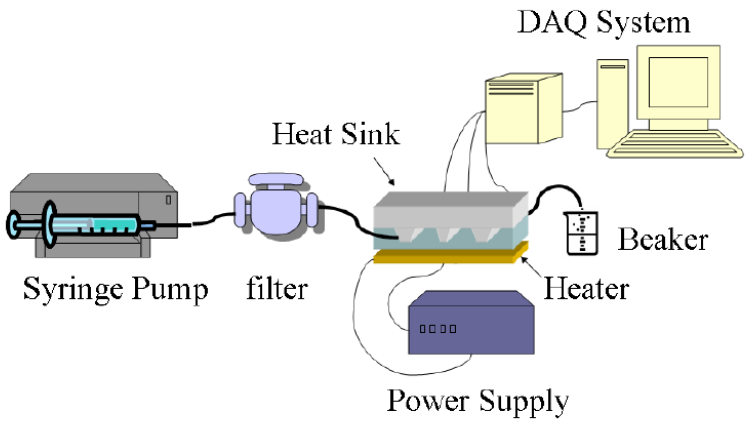

Figure 3.3: Schematic of the Experimental set up [17]

3.3.1 Data Acquisition System

All the temperature data were collected by data acquisition system which consists of SCXI- 1000 chassis, SCXI-1100 multiplexer module and the SCXI 1300 terminal block. PCI-604E DAQ card from National Instrument is used to connect with SCXI system to the terminal which in turn uses the Labview program to collect the data. The data acquisition system uses waves and signals to convert data from loop to the program. This type of data acquisition system can handle a variety of transducer inputs. That includes pressure transducers, thermocouples, and measurements in DC voltage, resistance and frequencies.

Figure 3.4 Picture of the DAQ system with SCXI Chassis and Multiplexer

3.3.2 Thermocouples

Thermocouples are used to measure the temperature drop across the heat sink at the Inlet and outlet. Also temperature of base of the heat sink was calculated by inserting three thermocouples at three different lengths L_1, L_2, L_3. The average value of these three readings would give us the mean temperature of the heat sink base. K-type thermocouples are used for this experiment. The K-type thermocouple uses Chromel alloy and Alumel alloy. These K-type thermocouples have a very wide operating range of -200 to 1250 °C. The K-type thermocouple has an accuracy of +/- 0.5 °C.

3.3.3 Syringe Pump

We used an Infuse/withdraw syringe pump PHD 2000 from Harvard apparatus to drive the flow. These pumps have RS-232 communication capabilities and they are programmable using the keypad. The programmable aspect of this pump allows us to use this as flow meter by controlling the flow rate and as a valve since a specific flow rates can be reached with continuous measurements. Distilled water is used as the coolant liquid due to its large heat capacity (4186 J/ kg K).

Figure 3.5 Picture of Syringe Pump (PHD 2000 Harvard Apparatus)

3.3.4 Heater

For experimental purpose, a kapton flexible silicone rubber heater SRFG-203 is used. The dimensions of the heater are 2 × 3 in. The watt density of the heater is 10 W/ in^2 and has a total ratted wattage of 60 W. The operating range for this particular heater model from Omega is -56 °C to 232 °C. These flexible heaters can improve heat transfer can speed warm-ups where controlled heating is required in confined areas. The Kapton heater is attached beneath the heat sink with high conductive epoxy to simulate heat released by electronic component. The epoxy used is Thermon T-99-1. It's a specialty heat transfer compound formulated to provide exceptional thermal stability and superior bonding. This epoxy is electrically nonconductive and has exceptional bond strength to resist thermal expansion and contraction. Three K-type thermocouples are different distance from the center of the heater are attached with the help of this epoxy for a better contact and more accurate readings.

Figure 3.6 Kapton Silicone Rubber Heater

3.3.5 Differential Pressure Transducer

Figure 3.7 Differential Transducer

Another important device in the loop is the pressure transducer. It is able to measure the pressure drop across the heat sink by differential pressure measurements. The transducer used for the loop is the PX154-001DI from Omega Engineering. Conversion of physical pressure into an electrical signal is achieved by physical deformation of the strain gauges which are bonded into the diaphragm of the pressure transducer and wired into a Wheatstone bridge configuration. Pressure produced to the pressure transducer produces a deflection of the diaphragm which introduces strain to the gauges. The strain produces an electrical resistance proportional to the pressure. This wet differential pressure transducer has range of 0- 1” Water column

3.3.6 Power supply

Figure 3.8 Picture of Variac Transformer

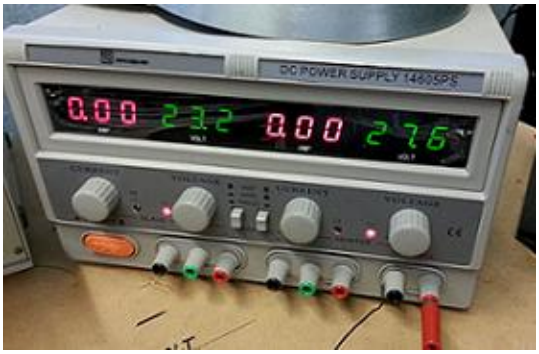

Figure 3.9 Picture of DC Voltage Supply

We used two different power supply for heater and differential pressure gauge. The resistance Kapton rubber heater is plugged with the variable transformer as show in picture 3.11. Since there's no temperature feedback controller used, we had to make use of Variac for constant heat flux condition to maintain the power of the heat source to generate heat to maintain steady temperature. The input voltage to the Variac is 120 V, 50/60 Hz frequency whereas the output is 120/140 V, 10 A and 1.4 KVA. It offers flexibility to step up the voltage from the supply voltage to higher voltages or we can step down voltage compared to the supply voltage. We can establish this operation by selecting the mode and then controlling the knob to select the needed voltage. We need an external DC power supply for the differential pressure transducer. As mentioned earlier we need a 24 VDC excitation voltage which would return an output voltage form 0-5 VDC which is then converted into corresponding pressure drop.

3.4 Experimental Procedure

3.4.1 Calibration and Data Collection

We had to calibrate certain data collecting devices before we begin running the experiment. All the K-type thermocouples were carefully calibrated in a water bath using 6-points calibration method. The coolant that is used in this study is distilled water, so the operating range is kept between 0 °C to 100 °C. The calibration data was recorded and piecewise linear curve was formed. Most of thermocouples showed an accuracy of +/- 0.5 °C. . The excitation voltage needed is 24 V DC from the power supply. We had to connect the higher of the two media pressures to port labeled “HIGH” and the lower of the two pressures to port labeled “LOW”. This transducer can be mounted in any position; however we should be careful to the moisture passing through non-waterproof electrical connectors. The zero and span may be adjusted if necessary or desirable; however the requested full scale range as shipped is established with fixed resistors minimizing the range of adjustment pots. The average full scale adjustability is approximately ± 10 % of the range shipped. After applying power allow approximately 20-30 minutes for signal to stabilize. When operating at very low differential pressures or in applications where the pressure is fluctuating rapidly, it is advisable to use “snubber” or air flow restrictors in the input lines. This steadies the output signal and keeps it from bouncing erratically.

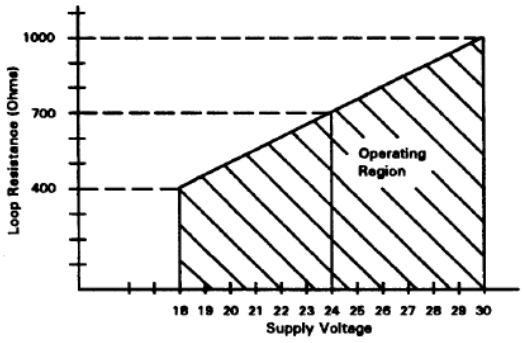

Figure 3.10 Operating range of the differential pressure transducer (Omega Engineering)

Non-Temperature Compensated Accuracy (All Output Signals)			
Span	Accuracy with Temperature Shift from 25 °C Ambient (% FS)		
	± 5°C	±10°C	± 25°C
0-27.7"WC	± .11%	± .32%	± 1.00%
0-25.0"WC	.12	.36	1.10
0-10.0"WC	.30	.90	2.28
0-5.0 "WC	.60	1.80	5.54
0-3.0 "WC	1.00	3.00	9.23
0-1.0 "WC	3.00	9.00	27.70

Figure 3.11 Temperature Zero and Span effects of the transducer (Omega Engineering)

The overall surface area of the heat sink remains the same for all the three configurations. Syringe pump was turned on before the DC power supply to the transducer. We had to wait to let the system run for a while to ensure bubble free channels without any leakage in the system. The heat sinks are closed with a cover made of acrylic material cut to the exact overall dimensions of the heat sink. We introduced a silicone rubber seal before using this cover over the heat sink, to make sure there's no leak when the flow from the syringe pump is turned. Following picture shows how this cover is bolted with the rubber seal and the heat sink substrate.

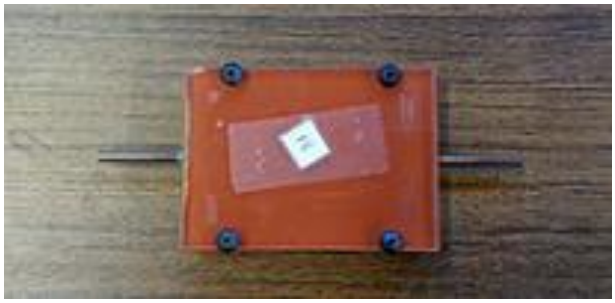

Figure 3.12 Picture showing the seal and cover for heat sink

There are two main categories of data involved in this study. Temperatures data and pressure drop from the inlet of the heat sink. There are multiple temperature data that was needed to perform the investigation of the heat sink configurations. Temperature from the heat sink itself forms a category and temperature data from the heaters helps us to main the constant heat flux condition throughout the observation. The k-type thermocouples connected to the heat sink at various points helps us analyze important heat transfer characteristics of the heat sink.

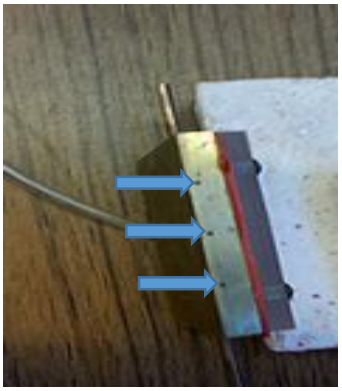

Figure 3.13 Picture showing slots to measure base temperature of heat sink

The above discussed picture shows the slots to measure the temperature of the heat sink at different heat flux conditions. It consists of three slots each 4 mm from the bottom of the substrate. We adopted and came up with such a design just to avoid any faulty readings when

the substrate is placed over the heat source. To differentiate the temperature readings of the heater and substrate this design proves more efficient. The average value of the three readings gives us the overall mean substrate temperature. The heater consists of three different thermocouples attached at different locations and the mean value of all the thermocouple readings gives us the temperature of the heater.

Figure 3.14 Picture showing Inlet/Outlet Temp measurement arrangement

This picture shows the scheme for measuring the inlet and outlet temperature of the working fluid (distilled water). The inlet and outlet water temperatures are measured by two K-type thermocouple probes inserted into the copper pipes connected to the heat sink. The differential pressure transducer is connected across the test section with a T- valve which bypasses the flow to the strain gauge. The test loop also contains a syringe pump at which we can program the needed flow rate eliminating the need for a flow meter. The range of the syringe pump is 0 to 190 ml/min. The pressure drop on mini scale is not significant and it becomes very low and virtually goes to zero when the flow rate is reduced below 150 ml/min. So the pressure drop readings are considered for data sets combined with the temperature readings only for flow ranging from 150 ml/min – 190 ml/min.

3.5 Experimental Uncertainty

Uncertainty analysis is a technique that was developed to validate the results obtained through any experimental investigation. A method developed by Kline and McClintock [13], was used here to estimate the uncertainties in experimental data. This method incorporates the estimated uncertainties in the experimental measurements i.e. coolant inlet and outlet temperatures, coolant flow rate, heat sink base temperature into the final parameters of interests like heat transfer rate, heat transfer coefficient and so on. Using the measured uncertainties of the above mentioned parameters, the maximum calculated uncertainties in heat transfer rate were found to be 6 %, 4.8 %, 4.5 % for the 4 mm, 3 mm and 2 mm channels respectively. The maximum uncertainty in overall heat transfer coefficient was about 4.7 % for all the three configurations. This is pretty much for the uncertainties corresponding to the temperature measurements. The maximum uncertainty observed with respect to the pressure drop measurements are nearly 9 %. The main reason for this uncertainty was because of the low resolution of the available transducer. There are not many commercial differential pressure transducers available for such low pressures of the order 0 to 0.10 inches of WC. That's one of the key observations for the uncertainty with respect to pressure drop measurements. Repeatability is an important factor as far as the uncertainty analyses in experiments are concerned. The repeatability of the pressure drop measured falls below 10 % and it agrees well with the theoretical pressure drop. Also the repeatability in temperature measurement techniques is also well maintained within 2-3 %.

Chapter 4 **Results and Discussion**

The experimental results obtained with the set up that was explained in the previous chapter are presented here. But before we present the results, dimensional quantities, dimensionless terms and data reduction calculation are introduced first. The experimental results with different geometry configurations will be presented at the later part of this chapter.

4.1 Hydraulic Parameters

Following are some the important parameters used commonly in fluid dynamics and heat transfer to describe pressure and heat transfer characteristics. Several definitions used in this study are as follows [2] [17]:

4.1.1 Theoretical Pressure Drop

It is important to understand how the theoretical pressure drop is calculated. It gives us a good idea about the trend and helps us compare the values obtained experimentally. Otherwise the pressure drop is estimated in order to select a pressure transducer of the appropriate conditions. The pressure drop is calculated by the following formula:

$$\Delta P = f_f \times \frac{L}{D} \times \rho \frac{V^2}{2}$$

Whereas

ΔP – Friction Pressure drop

L- Length of the channel (m)

D – Hydraulic diameter for rectangular channel (m)

ρ – Density of the liquid (996.59 kg/ m^3)

V- Velocity of the liquid (m/s) whereas, D = $\frac{4 \times a \times b}{2(a+b)}$

4.1.2 Friction Factor

The friction factor is defined as the ratio of wall shear stress τ to the kinetic energy per unit volume. The friction factor for a rectangular channel is given by the following formula

$$\mathbf{f_f} = \frac{\mathbf{64}}{\boldsymbol{Re}}$$

4.1.3 Reynolds Number

One of the dimensionless parameters that is very useful in this study is Reynolds number. It is given as the ratio of inertial forces to viscous forces.

$$\boldsymbol{Re} = \frac{\boldsymbol{v\,L}}{\boldsymbol{\vartheta}}$$

Whereas v – velocity of object relative to liquid, L- Hydraulic diameter, ϑ − Kinematic Viscosity

4.1.4 Euler Number

Euler number is a dimensionless number used in fluid flow calculations. It expresses the relationship between local pressure drop and the kinetic energy per unit volume. It is mainly used to characterize the losses in the flow, where a frictionless flow corresponds to an Euler number of 1.

$$Eu = \frac{P_{high} - P_{low}}{\rho\, V^2}$$

Whereas

P_{high} - Upstream Pressure of the fluid

P_{low} - Downstream Pressure of the fluid

V- Characteristic Velocity of the fluid

4.2 Heat Transfer Parameters

4.2.1 Heat Transfer Rate

The heat removed by the water circulating through the heat sink is calculated by applying the conservation of energy principle to control volume with one inlet and one exit, with no work interactions and assuming negligible changes in Kinetic and potential energies. This is expressed as

$$Q = m\, c_P\, (T_{out} - T_{in})$$

The thermos physical properties of water at mean fluid temperature are used in all of the calculations.

$$T_m = \frac{T_{in} + T_{out}}{2}$$

4.2.2 Heat Transfer Coefficient

The heat transfer coefficient is the heat transfer proportionality coefficient between the heat flux and thermodynamic driving force for the flow of heat which is the temperature difference. The overall heat transfer coefficient for each heat sink for every flow rate was calculated by applying the following equation.

$$Q = m\, c_P\, (T_{out} - T_{in}) = UA$$

$$U = m\, c_P \frac{(T_{out} - T_{in})}{A}$$

A- Area of heat sink, U- Overall Heat Transfer Coefficient

$$A = 2\,(\alpha \times \beta) + (c \times l)(n-1) + (h \times l \times 2)n + (t \times h \times 2)n$$

Table 4.1 Dimensions of the heat sinks (mm)

Length of channel (l)	50
Width of finned section()	40
Unfinned length ()	5
Height of fins (h)	4
Thickness of fins (t)	2
Overall thickness of base	8

4.2.3 Nusselt Number

Nusselt number is defined as the ratio of convective conductance to the pure molecular thermal conductance:

$$Nu_L = \frac{h\, D_h}{k}$$

Whereas

h- Convective heat transfer coefficient of fluid

k- Thermal conductivity of the fluid

4.3 **Results and discussion**

4.3.1 Fluid Performance

The fluid performance of the three different configurations of minichannel heat sinks is discussed here. This analysis includes the comparison of theoretical pressure drop calculated analytically with that of experimental pressure drop, Reynolds number with experimental pressure drop, comparison of theoretical and experimental pressure drop for three different configurations of heat sink 2 mm, 3 mm and 4 mm minichannel heat sinks at flow rates 190 ml/min, 175 ml/min and 150 ml/min. Like discussed before the pressure drop in mini scale is not as significant as in micro scale channels. So when the pressure drop for these channels virtually drop to zero and it is hard to record very small values of pressure drop due to the low resolution of the available differential pressure transducer. Also we have investigated some dimensionless parameters like Euler number which corresponds to the local pressure drop and kinetic energy per unit volume.

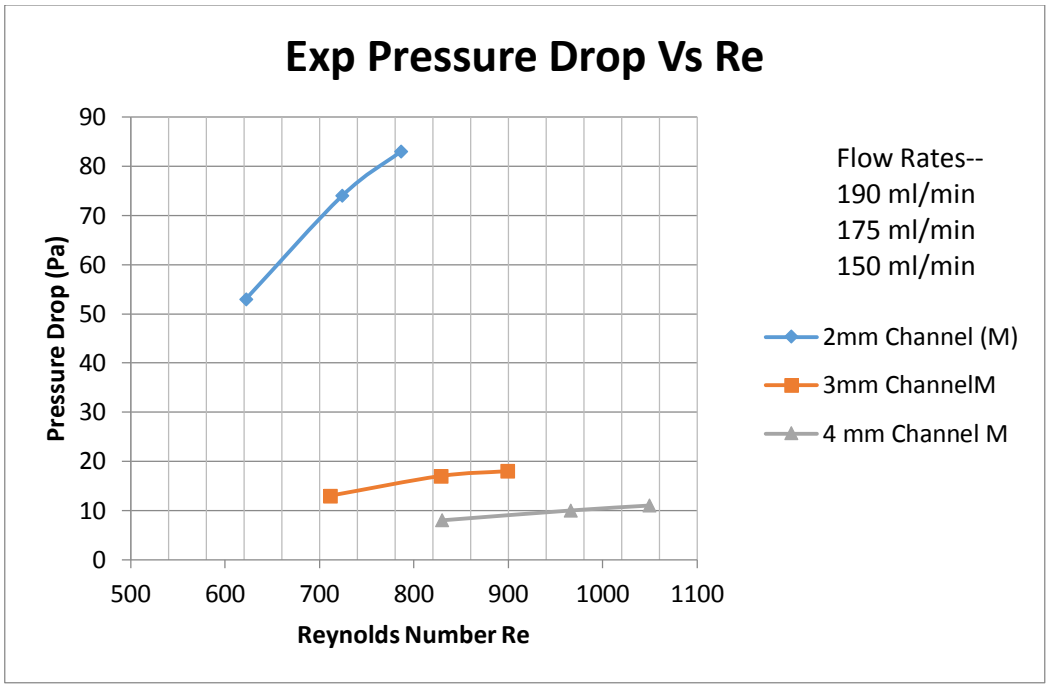

Figure 4.2 Variation of Experimental Pressure Drop (Vs) Reynolds Number

This analysis shows the variation of experimentally measured pressure drop and the Reynolds number. As we can see that the pressure drop in all three configuration has an increasing trend with increase in Reynolds number which is related to the flow rate. Pressure drop measured is maximum 83 Pa for the 2 mm minichannel heat sink. As the width or fin spacing increases the pressure drop value decreases and no pressure drop is virtually recorded with the omega transducer below the flow rate 150 ml/min for 3 mm and 4 mm minichannel heat sink. And the maximum range of the syringe pump is 190 ml/min which is why the experimental investigation on pressure drop was conducted on this flow rate range. When we compare this pressure drop value to micro channel heat sink we can conclude that the pressure drop in mini scale was not so significant when compared to micro or nano scale heat sinks. Also it is worthwhile comparing the experimental pressure drop results with the theoretical pressure drop to avoid any experimental uncertainty and anomaly.

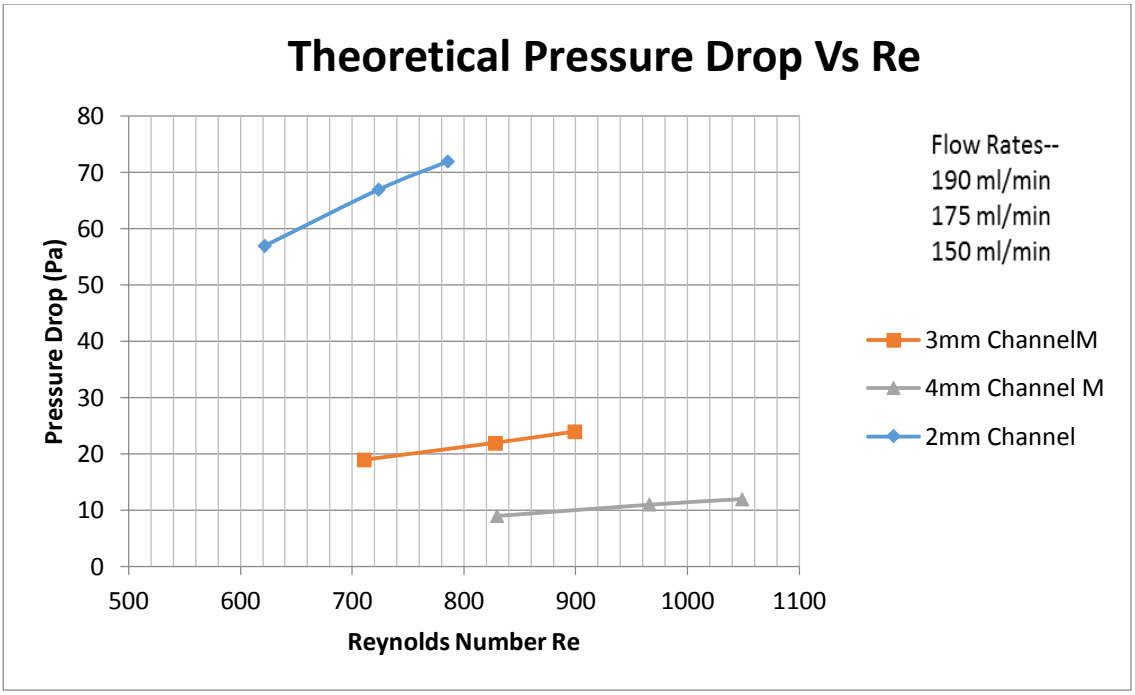

Figure 4.3 Variation of Theoretical Pressure Drop (Vs) Reynolds Number

The figure 4.3 shows the variation of theoretically calculated pressure drop with Reynolds number. Like discussed before these values serves as validation for the experimental result. The maximum pressure drop of 73 Pa occurs at a flow rate of 190 ml/min and the trend of the pressure drop for all the three configurations shows similar trend. Pressure drop increases with increase in flow rate and 4 mm minichannel heat sink offers the lowest pressure friction loss of all the three configurations and below flow rate 150 ml/ min, the pressure drop value approaches zero. Also it is important to note that the pressure associated with the distribution of the coolant to the inlet reservoir and outlet reservoir may influence the experimental accuracy. The discrepancy in experimental measurement also depends on fluid connections and manifold assembly like snubber that was included in the measuring line. A comparison figure for

the theoretical and experimental pressure drop with the respect to Reynolds number is given below.

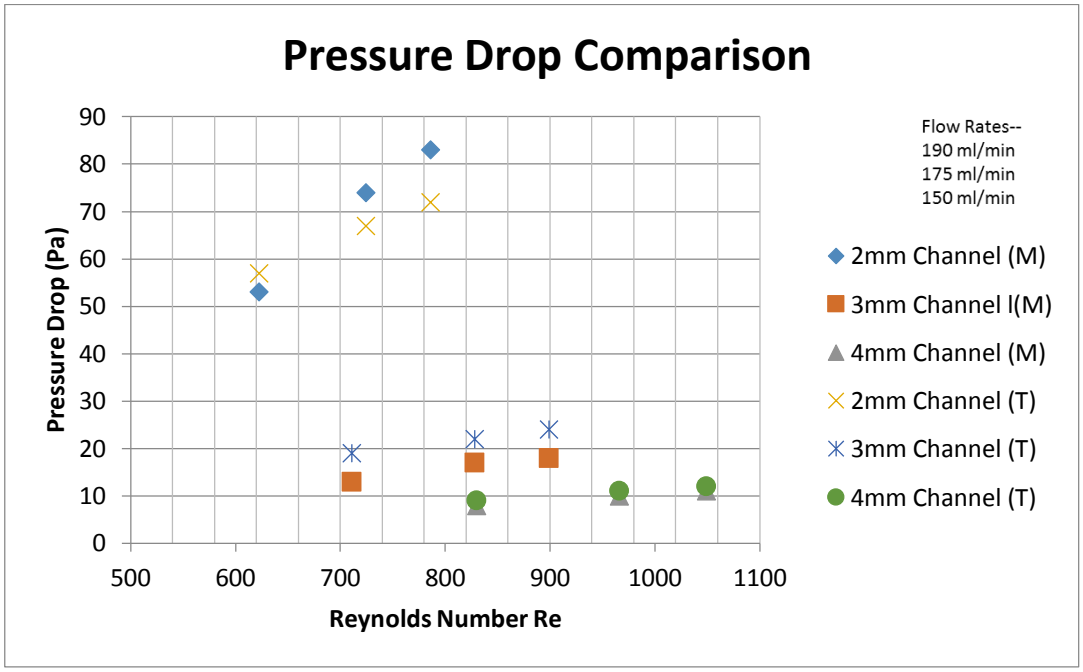

Figure 4.4 Comparison of theoretical and experimental pressure drop against Reynolds number

This figure shows the overlap of the theoretical and experimental pressure drop. 'T'- denotes theoretical and 'M'- denotes the measured experimental values. It was quite evident that theoretical pressure drop values falls within 10 % error of the measured experimental value. The experimental pressure drop was comparatively greater than the theoretical pressure drop values for 2 mm minichannel heat sink. Whereas the experimental pressure drop values for the 3 mm and 4 mm channel is less than the theoretical values. This behavior accounts to the limited resolution of the omega pressure transducer that was used. Several set of pressure drop readings were taken and average value was taken just to reduce the error margin. This method

proves quite effective as we can see that the theoretical pressure drop values are well in agreement with the experimental values.

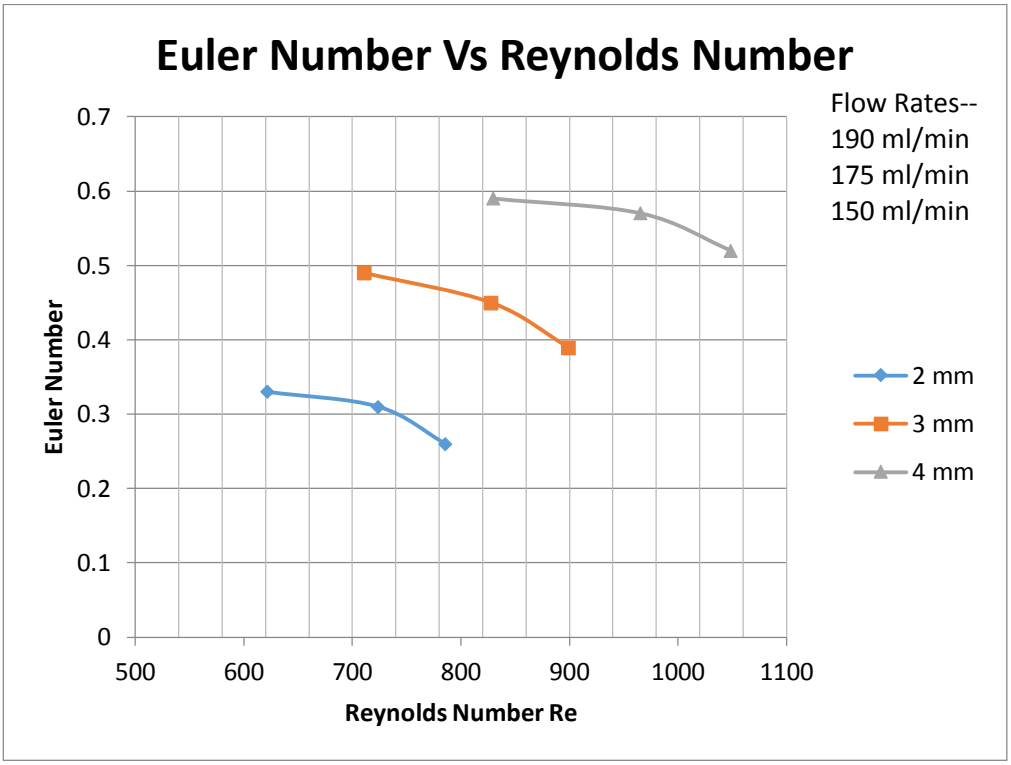

Figure 4.5 Euler Number against Reynolds Number

The dimensionless pressure drop is Euler number. The graph above shows the variation of the dimensionless term with Reynolds number with respect to flow rates 190 ml/min, 175 ml/min and 150 ml/min. Euler number provides similar information as that of a friction factor with constant properties and fixed channel dimensions [17]. Euler number usually corresponds to smaller friction factor decreases with increase in Reynolds number. Eventually with increase in Reynolds number the decreasing rate is dropping but unfortunately we don't have enough pressure drop data to showcase this trend in this investigation.

4.2.3 Thermal Performance

In this experiment the heater is attached to the bottom of the heat sink. The working liquid used in this investigation was distilled water which is pumped into the mini channel heat sink with syringe pump. This working liquid takes away the heat from and exit from the outlet to the beaker. Three thermocouples were attached to the top of the heater with high conductive epoxy paste. The average temperature of these three readings is taken as the temperature of the heater. Two separate thermocouples are used to measure the temperature of the inlet coolant liquid and outlet temperature of the coolant. Apart from these we have three slots at one side of the heat sink base which was useful to measure the base temperature of the heat sink.

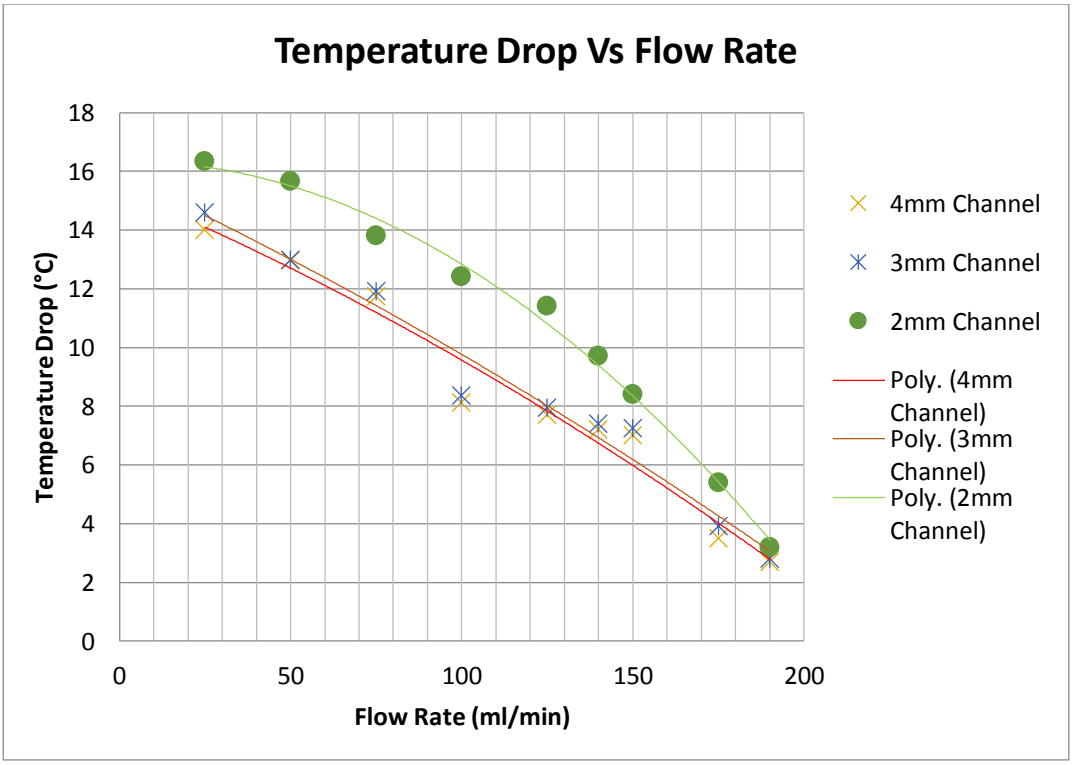

Figure 4.6 Comparison of Temperature drop with Volumetric Flow rate

The temperature drop is measured by measuring the difference between temperature of the coolant liquid at the outlet and inlet. The figure 4.6 shows the temperature drop for three different heat sinks with respect to the volumetric flow rate. The processor heat was simulated by the heater attached to the bottom of the heat sink. The greatest temperature drop was observed when a 2 mm fin spacing heat sink was used. Temperature drop of 16.4 °C was observed with 2 mm fin spacing with 25 ml/min volumetric flow rate. The performance of the other two configuration of heat sinks are quite close and temperature drop achieved by 3 mm and 4 mm channel falls below the performance of the 2 mm heat sink for the same volumetric flow rate.

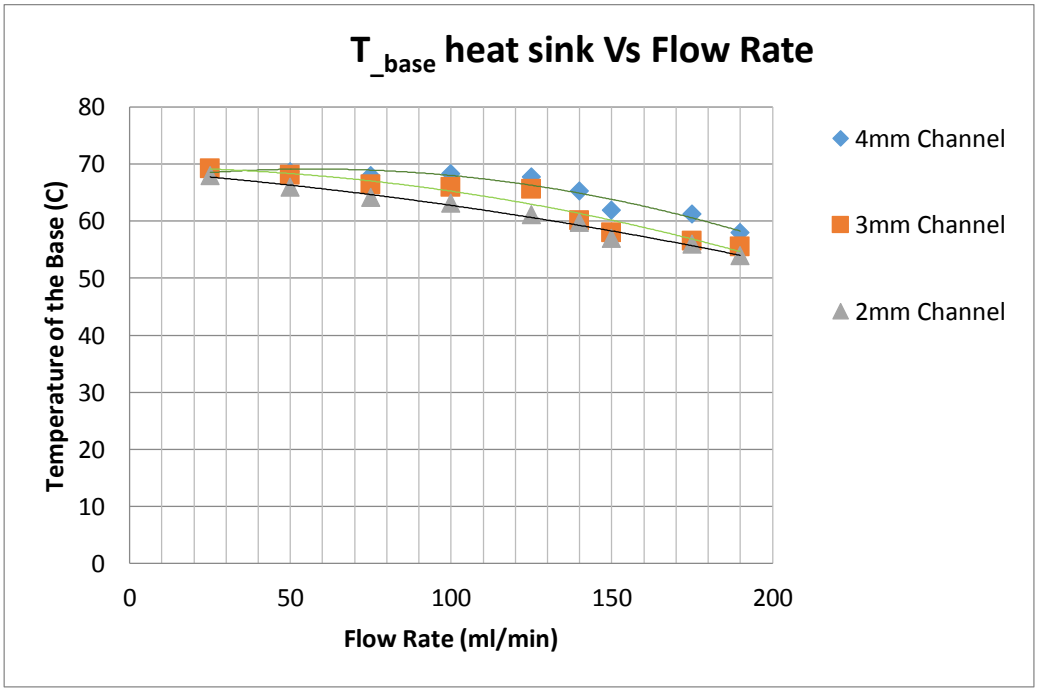

Figure 4.7 Variation of Base temperature of heat sink with flow rate

The base temperature of the heat sink was analogous to the processor operating operator under varying loading conditions. Figure 4.7 shows the variation of base temperature with the flow rate of water circulating through the three heat sink geometries. For all the three geometries the base temperature reduces by increasing the flow rate of the coolant through the heat sink. The base temperature drops considerably with heat sink 2 mm than the other two configurations. Decreasing the fin spacing considerably reduces the effect of flow rates on base temperature (lower Reynolds number). For instance changing the flow rate from 25 ml/min to 190 ml/min produces a drop in base temperature 16 °C. The present geometries give good comparison for the effect of fin spacing on base temperature with respect to flow rate. Thermal performance of 3 mm and 4 mm channel was quite similar and it is quite on the higher end.

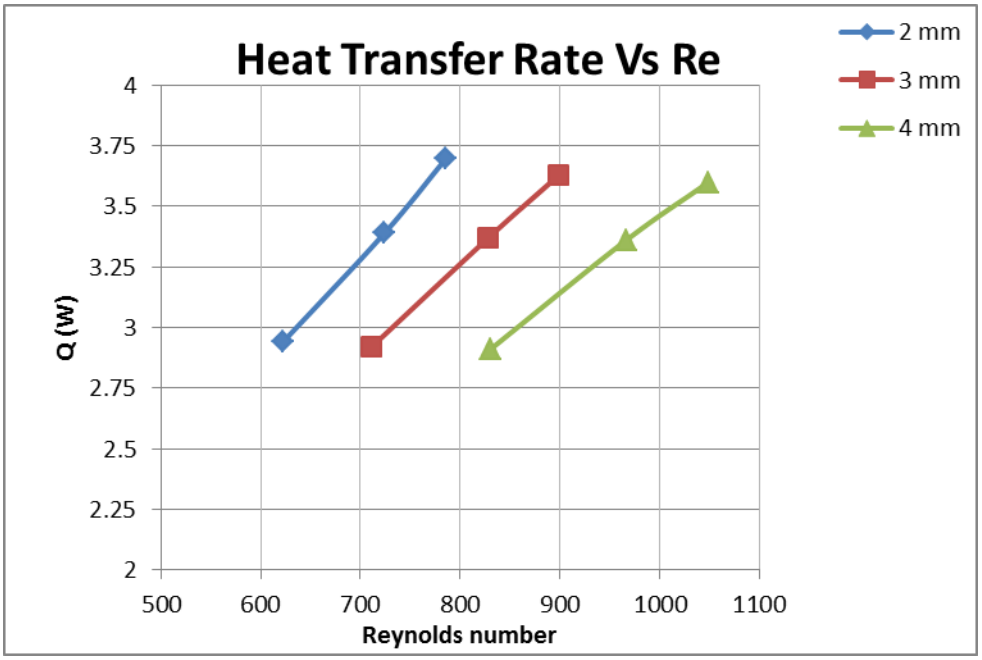

Figure 4.8 Variation of heat Transfer Rate with Reynolds Number

Figure 4.8 shows the comparison of heat transfer rate of the coolant with respect to the Reynolds number as a function of fin spacing. Despite the smaller values of Reynolds number for

finned heat sinks they showed significantly higher heat transfer rates which was due to the fact of significant area enhancement. It is evident that a finned heat sink with fin spacing of 2 mm at a Reynolds number of 622 was able to remove 3.7 W of heat which is nearly 31 % of the total power supplied. The error in total supplied is always found to be below 6 % of heat absorbed by the coolant plus heat loss to the outside air from the heating section.

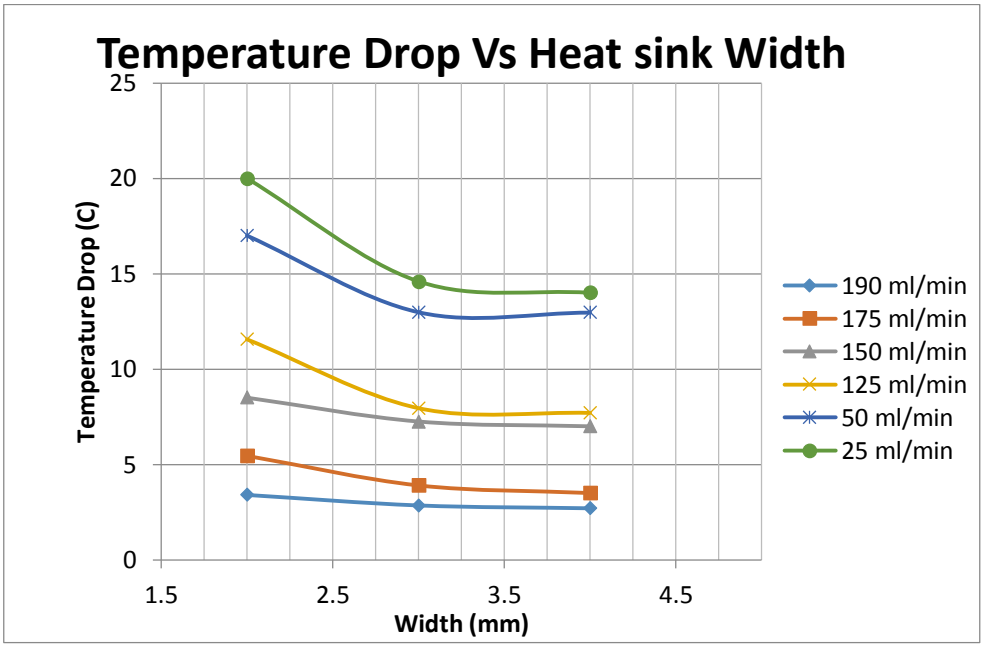

Figure 4.9 Variation of Temperature Drop (Vs) Width or fin spacing of heat sinks

The next investigation was carried on the variation of Temperature drop with fin spacing or width of the channels with respect to flow rate. This analysis was done from the temperature drop data obtained with flow rates ranging from 25 ml/min to 190 ml/min. As we can see from this figure that the temperature drop with fin spacing 2 mm with 25 ml/min is the greatest which is almost like 20 °C. Nevertheless the temperature drop of 3 mm and 4 mm are close and comparable to each other. Effect of fin spacing can be understood from this plot. Temperature drop decreases with increase in width at a particular flow rate.

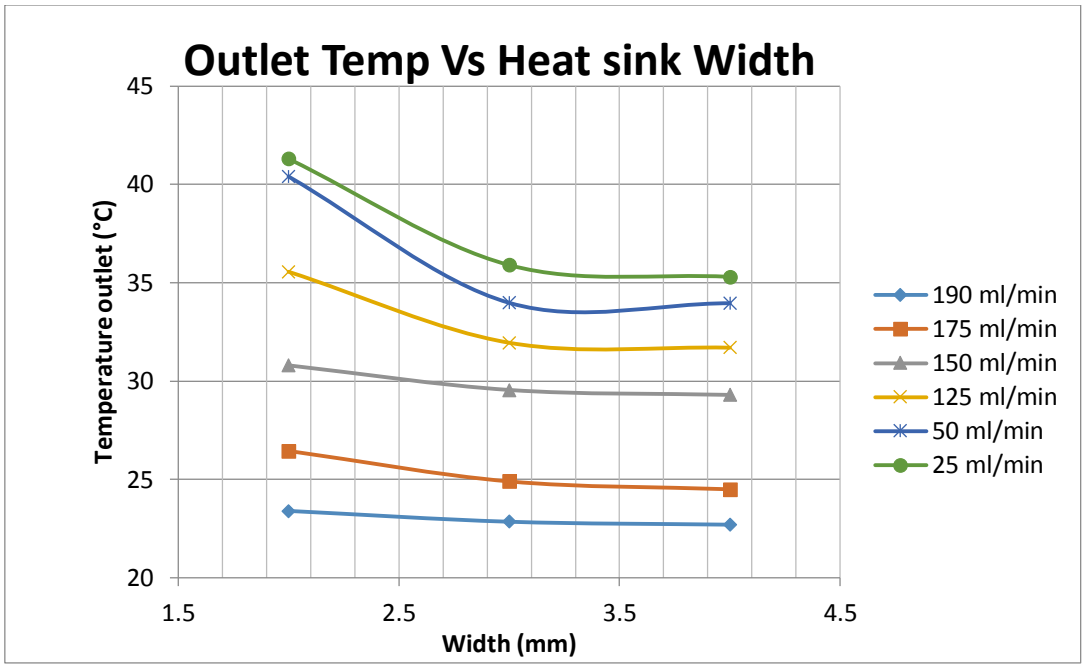

Figure 4.10 Variation of Outlet temperatures (Vs) Width of heat sinks

Another important parameter to be analyzed was the variation of outlet temperature with respect to the fin spacing or width of the channel. The higher the temperature at the outlet denotes more heat is removed. As we can see from the trend that it is similar to the previous plot on temperature drop with respect to fin spacing. This plot gives us similar information like the former. Increase in width of fin spacing provides gives low outlet temperature. The higher the temperature more efficient the heat sink is. As it is evident that outlet temperature for the heat sink 2 mm with respect to flow rate 25 ml/min is the highest (42 °C). The outlet temperature increases with decrease in flow rate for all the three configurations of heat sinks with 2 mm having the superior performance followed by 3 mm heat sink and 4 mm respectively.

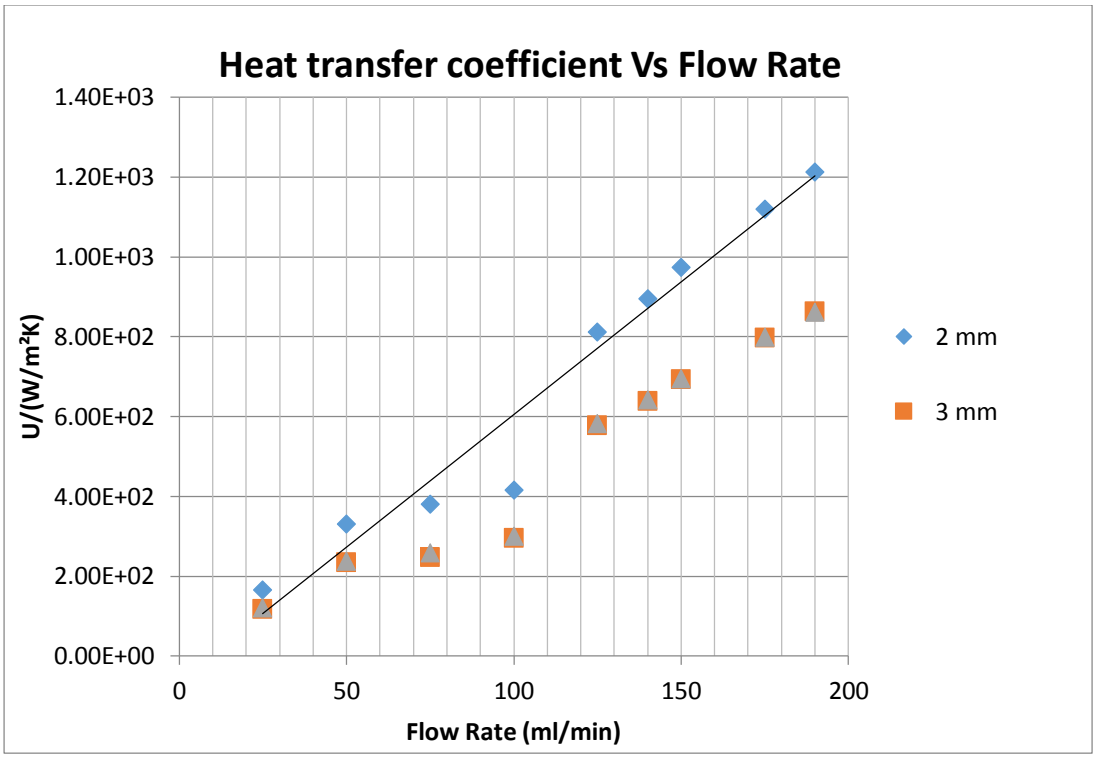

Figure 4.11 Variation of Overall heat Transfer Coefficient (Vs) Volumetric flow rate

The above graph shows the overall heat transfer coefficient with variation in volumetric flow rate of water for all three heat sinks. The maximum value of overall heat transfer coefficient was found as 1200 W/ m^2 K at a volume flow rate of 190 ml/min corresponding to the 2 mm heat sink. It can shown from the overall trend that the heat transfer coefficient increases with decreasing fin spacing. The trend line for the 2 mm heat sink for overall heat transfer coefficient was higher than the other two geometries. . This is due to the fact of largest heat transfer area for this particular geometry of heat sink. Whereas the trend for the 3 mm and 4 mm heat sinks are pretty close as far as the overall heat transfer coefficient is concerned.

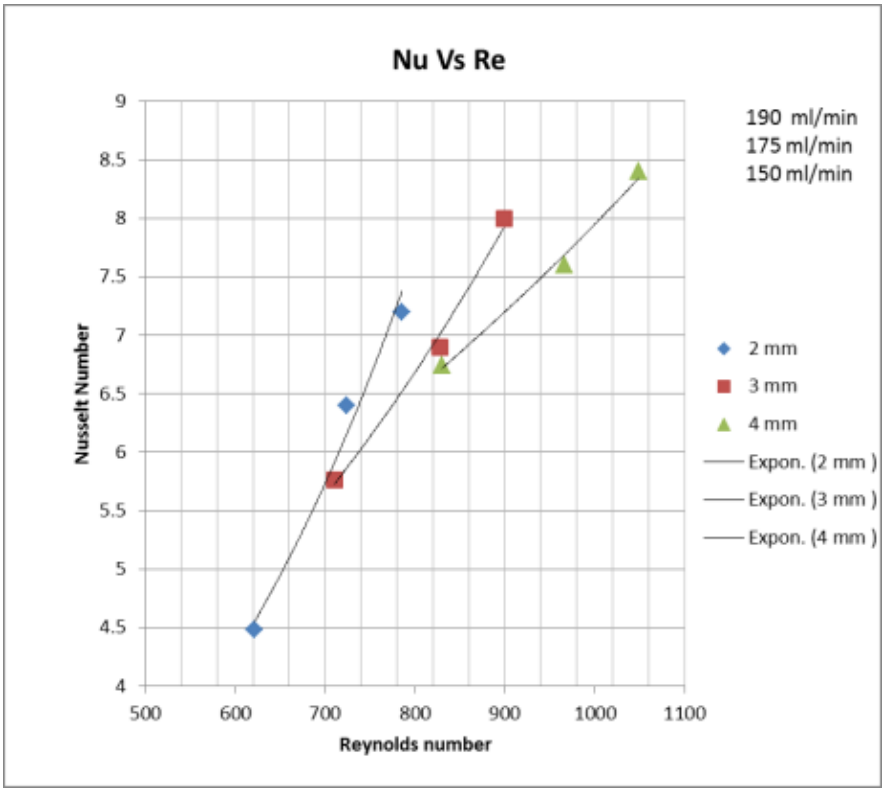

Figure 4.12 Nusselt Number (Vs) Reynolds Number

The final investigation was carried out on the dimensionless parameters to understand the thermal performance of the heat sinks that are considered for this study. This is an interesting observation because it shows which mode of heat transfer is dominant in the heat sink with respect to the flow rate. As we already know that the working liquid is distilled water used with copper heat sink with different sets of fin spacing so it is important to analyze which of mode of heat transfer is dominant in different geometries. As we can see that Nusselt number is larger for heat sink with fin spacing of 4 mm which denotes that convection was dominant with greater fin spacing. Whereas the Nusselt number is comparatively low in the 2 mm heat sink which shows that conduction is more dominant than convection in the reduced fin spacing. This concept also contributes the effect of fin spacing. The number of fins in 4 mm channel is 6

whereas the number of fins in a 2 mm channel is 9. Therefore increase in number of fins increases heat transfer by conduction. Whereas in 4 mm channel due to less number of channels convection through the coolant liquid was more dominant. The Nusselt number for a rectangular duct is given by the Dharaiya and Kandlikar equation given below:

$Nu = [(1.6980 \times 10^{-4})\ \alpha^6 - (5.7050 \times 10^{-3})\ \alpha^5 + (7.5552 \times 10^{-2})\ \alpha^4 - (0.5054)\ \alpha^3 + (1.8448)\alpha^2 - (3.8559)\ \alpha + 5.2720]$

The maximum deviation of Nusselt number data is ±9.5 % from the values predicted by the above equation.

Chapter 5 **Conclusions**

This chapter reviews the major conclusion from this experimental study. Electronic cooling problem on a mini scale was designed and studied.

The first part of the study we discussed about the design aspect from previous studies. It is important to understand the fabrication constraints before completing a design. This stage gives us the robustness to make quick changes to configuration before we do any fabrication. The material selection process was explained with properties and reasoning for choosing a heat sink from fabrication stand point. Three different heat sinks with spacing 2 mm, 3 mm and 4 mm are designed and fabricated using the milling process. The fabrication process was explained briefly for a basic understanding.

Experimental set up and procedure is briefly explained in chapter 3. This chapter includes brief introduction to all the components that was used in the experiment. Calibration procedure, data collection procedure was explained. Then overall assembly diagram was discussed. Procedure showing how to measure the temperature from the base of the heat sink, inlet and outlet are discussed. Pressure drop measurements and set up around was explained. Uncertainty analysis was discussed briefly.

Several parameters for analyzing the fluid performance and thermal performance was briefly introduced. Several dimensional and dimensionless terms were discussed. Measured pressure drop was analyzed against different flow rates. The conclusion being pressure drop was higher in 2 mm channel which was about 82 Pa. As the flow rate decreases the pressure drop values decreased and for a 4 mm channel pressure was approaching zero below 150 ml/ min volume

flow rate. Then this experimental value of the pressure drop was compared with the theoretical pressure drop. Variation of dimensionless pressure drop or Euler number over Reynolds number was explained. Thermal performance of the heat sinks are measured by various temperature readings from the experiments conducted. Variation of temperature drop across the heat sink with volume flow rate for a given heat sink configuration. It was shown that 2 mm heat sink has the maximum temperature drop 17-20 °C for a given flow rate of 25 ml/min which proves to be the most efficient configuration of all three. Next the heat sink base temperature was analyzed with flow rate for a given fin spacing. The temperature of the heat sink base was lowest in 2 mm configuration which again proves that 2 mm heat fin is more efficient than other two configurations. Then heat transfer parameters like heat transfer rate was analyzed. It was shown that 2 mm heat sink was able to remove 31 % of heat that was supplied to corresponding Reynolds number of 786 approximately. Then variation of outlet temperature and temperature drop with respect to fin spacing for a given volumetric flow rate was discussed. Then heat transfer coefficient with flow rate was discussed. From the trend discussed heat transfer coefficient increases with decreasing fin spacing. It was found that maximum overall heat transfer coefficient was 1200 W/ m^2 K for 2 mm fin spacing at 190 ml/min. Finally the effect of Nusselt number was discussed. This study helps us understand that importance to turn the focus on conventional manufacturing techniques for developing efficient heat sinks with simple geometry and simple working fluids.

Future Work

With the advancement in milling techniques and tool material with smaller sizes, this study provides ample scope to fabricate channels with lesser dimensions than those that was dealt in this study. Smaller fin spacing such as 1.5 mm, 1 mm, 0.5 mm can be explored with different

working fluids like ethyl alcohol and so on. It is more convenient to perform Numerical analysis on the sizes explored in this study and for reduced width, so that we can get a better idea if it's worth exploring material that can be machined with such precision using conventional technique. Another interesting study would be to consider aluminum heat sinks with working fluid such as glycol and dielectric fluids like Fluorinert, PAO with similar design and experimental criteria and numerical analysis with aluminum substrate would help us validate our results. So this study urge the manufacturers to focus on exploiting the heat transfer capabilities of enhanced geometries used with normal liquids despite using nanofluids whose performance is still ambiguous due to issues like deposition, agglomeration, maintenance cost associate by using them.

BIBLIOGRAPHY

[1]X.L. Xie, W.Q, Tao, Y.L He," Numerical study of turbulent heat transfer and pressure drop characteristics in a water cooled minichannel heat sink", J. Electronic Package. 129(2007) issue 247-255.

[2]Saad Ayub Jajja., Wajahad Ali, Hafiz Muhammad Ali, Aysha Maryam Ali (2013). "Water cooled minichannel heat sinks for microprocessor cooling: Effect of fin spacing" Applied Thermal Engineering 1359-4311.

[3]B.P Whelan, R. Kempers, A.J Robinson(2012), A liquid-based system for CPU cooling implementing a jet array impingement waterblock and a tube array remote heat exchanger, Appl. Therm. Eng. 39, 86-94.

[4]P. Naphon, S. Wongwises, (2010). Investigation on the jet liquid impingement heat transfer for the central processing unit of personal computers, Intl Journal of HMT 37 issue 822-826.

[5]C. bower, A. Ortega, P. Skandakumaran, R. Vaidyanatha, C. Green., T. Philips (2003). Heat transfer in water cooled silicon carbide milli-channel heat sinks for high power electronic applications.

[6]J.A. Eastman, S.U.S Choi, S. Li, W. Yu, L. Thompson (2001) "Anomalously increased effective thermal conductivities of ethylene glycol based nano fluids containing copper nanoparticles", Appl. Physics Lett. 78-718.

[7]N. A. Roberts, D.G. Walker (2010). "Convective performance of Nano fluids in commercial electronics cooling application", Appl. Thermal Engineering 1501-1506.

[8]C.T Nguyen, G. Roy, C. Gauthier, N. Galanis (2007). "Heat transfer enhancement using Al_2O_3-water nano fluid for an electronic liquid cooling system". Appl. Therm. Eng. 27 1501-1506

[9]C.T Nguyen, G. Roy, P.R. Lajoie, S.E.B. Maiga (2005). "Nanofluids heat transfer performance for cooling of high heat output microprocessor". In:Proceedings of the third IASME/WSEAS International conference on heat transfer, Thermal Engineering and Environment, Greece, pp. 160-165.

[10]H.B. Ma, C. Wilson, Borg Meyer, K. Park, Q, Yu, et al.," Effect of nanofluids on the heat transport capability in an oscillating heat pipe, Appl. Phys. Lett. 88 (2006) 143116.

[11]M. Rafati, A.A. Hamidi, M.S. Niaser," Applications of nanofluids in computer cooling systems", Appl. Them. Eng. 45-46(2012) 9-14.

[12]L. Godson, B. Raja, D. Mohan Lal, S. Wongwises, "Enhancement of heat transfer using nanofluids- an overview", Renew, sustain. Energy reviews 14 (2010) 629-641.

[13]S.J. Kline, F.A. McClintock, "Describing uncertainties in single-sample experiments", Mech Eng. 75 (1953) 3-8.

[14]M. B. Bowers, I. Mudawar, "Two-phase Electronic cooling using Mini-channel and Micro-channel Heat sinks: Part 2- Flow rate and pressure drop constraints" 298/ vol. 116 (1994) ASME.

[15]B. Shao, L. Wang, H. Chen, J. Li, "Optimization and Numerical Simulation of Multi-layer Microchannel Heat sink", International Conference on advances in Computational Modeling and Simulation. 1877-7058 (2011) Published by Elsevier Ltd.

[16]Sun, Zhanyu and Jaluria, Yogesh (2009) "Numerical Modeling of Pressure Driven Nitrogen slip flow in long rectangular Microchannels"", Part A: Applications, 56: 7, 541-562.

[17]J. Zhang, Y. Jaluria, S. Prakash, L. Lin (2010)," An experimental study on the effect of configuration of multiple microchannels on heat removal for electronic cooling", Proceedings of the IHTC-14.

[18]T. Icoz, N. Verma, Y. Jaluria (2006) " Design of Air and Liquid Cooling systems for Electronic Components using concurrent simulation and Experiment", 466 Vol. 128, Trans. ASME.

[19]Incropera, F. P., 1988, "Convection Heat Transfer in Electronic Equipment Cooling," ASME J. Heat Transfer, 110, pp. 1097-1111.

[20]A. Conti, G. Lorenzini, Y. Jaluria, "Transient Conjugate heat transfer in straight microchannels". 0017-9310. IJHMT- 55 (2012) 7532-7543.

[21]M.R.O Panao, Guerreiro, Moreira, “Microprocessor cooling based on an intermittent multijet spray system”. Volume 55, Issue 11-12, IJHMT (2012) 2854-2863.

[22]Fox, Robert and McDonald, Alan “Introduction to Fluid Mechanics” John Wily & Sons, Inc. New York pp 38-41

[23]Engineeringtoolbox.com/Moody chart

[24]V.V. Dharaiya, S.G. Kandlikar, “Numerical Investigation of Heat Transfer in Rectangular Microchannels under H2 Boundary conditions During Developing and Fully Developed Laminar Flow”, ASME 2012.

[25]PowerMill/Cad/cam Manual pdf